Department of Applied Mechanics

Effect of cell structure geometric and elastic parameters on wood rigidity

Johanna Sjölund

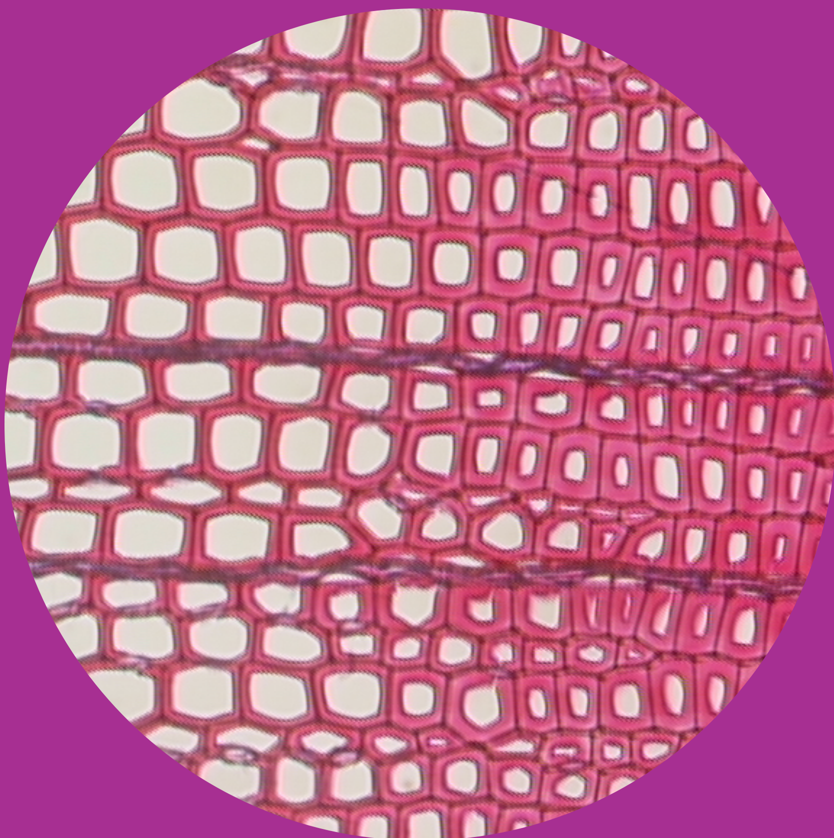

Aalto University

DOCTORAL DISSERTATIONS

Aalto University publication series
DOCTORAL DISSERTATIONS 38/2015

Effect of cell structure geometric and elastic parameters on wood rigidity

Johanna Sjölund

A doctoral dissertation completed for the degree of Doctor of Science (Technology) to be defended, with the permission of the Aalto University School of Engineering, at a public examination held at the lecture hall 216 of the school on 24 April 2015 at 12.

Aalto University
School of Engineering
Department of Applied Mechanics
Mechanics of Materials

Supervising professor
Prof. Jukka Tuhkuri

Thesis advisor
D.Sc. Jouni Freund

Preliminary examiners
Prof. Josef Eberhardsteiner, Vienna University of Technology, Austria
PhD Stefania Fortino, VTT, Finland

Opponent
Prof. Peter Niemz, ETH Zurich, Switzerland

Aalto University publication series
DOCTORAL DISSERTATIONS 38/2015

ISBN 978-952-60-6132-0 (printed)
ISBN 978-952-60-6133-7 (pdf)
ISSN-L 1799-4934
ISSN 1799-4934 (printed)
ISSN 1799-4942 (pdf)
http://urn.fi/URN:ISBN:978-952-60-6133-7

Unigrafia Oy
Helsinki 2015

Finland

NORDIC ECOLABEL
441 697
Printed matter

Aalto University

Abstract

Aalto University, P.O. Box 11000, FI-00076 Aalto www.aalto.fi

Author
Johanna Sjölund

Name of the doctoral dissertation
Effect of cell structure geometric and elastic parameters on wood rigidity

Publisher School of Engineering

Unit Department of Applied Mechanics

Series Aalto University publication series DOCTORAL DISSERTATIONS 38/2015

Field of research Mechanics of Materials

Manuscript submitted 15 December 2014 **Date of the defence** 24 April 2015

Permission to publish granted (date) 17 February 2015 **Language** English

☐ **Monograph** ☒ **Article dissertation (summary + original articles)**

Abstract

Cellular materials, for example wood and Nomex, are widely used in different applications, ranging from construction to pulping and scales ranging from millimetres to hundreds of meters. As a natural material wood is inherently orthotropic and inhomogeneous. The cell structure of wood consists of long cells, which have random variation of shape and size, but also directed variation of cell shape and size due to the growth ring.

Physical experiments on rigidity are not capable of explaining the relative effects of individual features, as only a general idea of the behaviour of a material can be determined. This is due to the physical experiments being limited by the specimen size and type.

Simulation experiments based on micromechanical modeling give additional freedom of design and different features can be considered individually. A simulation experiment on rigidity has design like a physical experiment where a specimen is subjected to stress and the corresponding strain is obtained by direct measurement. Simulation on a cellular structure requires knowledge not only on the

effect of the important features but also of the features that are left out.

The rigidity of cellular material depends on geometry of the cell structure, thickness of a cell wall and elastic properties of a cell wall. A geometric model is needed to describe the geometry of the cell structure. As natural materials have variations in the geometry which affect the rigidity of a structure, the variations need to be included in the model.

Variation in the features can be included by modeling non-regular specimens. A regular structure can be considered by means of computational homogenization.

Nomex is used as a simplified model of wood for which both physical and simulation experiments are possible. The beam model is validated for thin cell walls by comparing the results of two different cell geometries.

The relative effect of different geometric and material features on rigidity of spruce is quantified, which gives insight into their importance. The effect of variations is quantified in spruce earlywood. A model is developed that can be used to calculate the effective rigidity for any combination of the features. The effect of selected features on rigidity is illustrated.

Keywords Cellular materials, Wood, Spruce, Nomex, Micromechanical modeling, Computational homogenization, Rigidity

ISBN (printed) 978-952-60-6132-0 **ISBN (pdf)** 978-952-60-6133-7

ISSN-L 1799-4934 **ISSN (printed)** 1799-4934 **ISSN (pdf)** 1799-4942

Location of publisher Helsinki **Location of printing** Helsinki **Year** 2015

Pages 124 **urn** http://urn.fi/URN:ISBN:978-952-60-6133-7

Aalto-yliopisto

Tiivistelmä

Aalto-yliopisto, PL 11000, 00076 Aalto www.aalto.fi

Tekijä
Johanna Sjölund

Väitöskirjan nimi
Geometrian ja materiaaliparametrien vaikutus puun jäykkyyteen

Julkaisija Insinööritieteiden korkeakoulu

Yksikkö Sovelletun mekaniikan laitos

Sarja Aalto University publication series DOCTORAL DISSERTATIONS 38/2015

Tutkimusala Lujuusoppi

Käsikirjoituksen pvm 15.12.2014 **Väitöspäivä** 24.04.2015

Julkaisuluvan myöntämispäivä 17.02.2015 **Kieli** Englanti

☐ **Monografia** ☒ **Yhdistelmäväitöskirja (yhteenveto-osa + erillisartikkelit)**

Tiivistelmä

Solumaisia rakenteita, kuten puuta tai Nomexia, käytetään useissa erilaisissa sovelluksissa, aina rakentamisesta sellunkeittoon ja erilaisissa skaaloissa, millimetreistä aina satoihin metreihin. Luonnollisena materiaalina puu on ortotrooppinen ja epähomogeeninen. Puun solurakenne koostuu pitkänomaisista soluista, joilla muoto ja koko vaihtelevat sekä satunnaisesti että järjestäytyneesti kuten vuosirenkaassa.

Fysikaalissa kokeissa saadaan yleinen käsitys materiaalin käyttäytymisestä, mutta ei saada tietoa yksittäisten ominaisuuksien vaikutuksista, koska sekä koekappaleen koko että tyyppi ovat rajoitettuja.

Simulaatiokokeilla, jotka perustuvat mikromekaaniseen mallinnukseen, on suurempi vapausaste ja erilaisia ominaisuuksia voidaan käsitellä yksittäin. Simulaatiokokeet suunnitellaan vastaamaan fyysikaalisia kokeita, joissa näytettä kuormitetaan ja venymä mitataan suoraan. Simulaatioita varten on tiedettävä sekä tärkeiden ominaisuuksien vaikutukset jäykkyyteen että pois jätettävien ominaisuuksien vaikutukset.

Puun jäykkyys riippuu solurakenteen geometriasta, soluseinämän paksuudesta ja soluseinämän materiaaliominaisuuksista. Geometrisen mallin avulla voidaan kuvata solurakennetta. Variaatioita on käsiteltävä mallissa, koska luonnollisissa materiaaleissa esiintyvä geometrian variaatio vaikuttaa myös rakenteen jäykkyyteen.

Ominaisuuksien variaatiota voidaan tutkia mallintamalla epäsäännöllisia rakenteita. Säännöllistä rakennetta voidaan mallintaa laskennallisen homogenisaation avulla.

Nomexia käytettiin puun yksinkertaistettuna mallina, jolle oli mahdollista suorittaa sekä fyysikaalisia kokeita, että simulaatiokokeita. Ohuiden seinämien palkkimalli osoitettiin oikeaksi vertaamalla kahden eri rakenteen tuloksia.

Eri geometria- ja materiaaliominaisuuksien variaation vaikutus kuusen jäykkyyteen voidaan määrittää ja tällöin ominaisuuksien suhteellinen merkittävyys voidaan arvioida. Kehitetyn tietokonemallin avulla voidaan laskea efektiivinen jäykkyys mille tahansa ominaisuuksien yhdistelmälle. Valikoitujen ominaisuuksien vaikutusta jäykkyyteen havainnollistetaan kuvaajien avulla.

Avainsanat Solurakenteiset materiaalit, Puu, Kuusi, Nomex, Mikromekaaninen mallintaminen, Laskennallinen Homogenisointi, Jäykkyys

ISBN (painettu) 978-952-60-6132-0 **ISBN (pdf)** 978-952-60-6133-7

ISSN-L 1799-4934 **ISSN (painettu)** 1799-4934 **ISSN (pdf)** 1799-4942

Julkaisupaikka Helsinki **Painopaikka** Helsinki **Vuosi** 2015

Sivumäärä 124 **urn** http://urn.fi/URN:ISBN:978-952-60-6133-7

Preface

The research leading to this thesis was conducted in the Department of Applied Mechanics in Aalto University. The research was part of project Energy Efficient Wood Processing and Machining (E-wood) supported by Multidisciplinary Institute of Digitalisation and Energy (MIDE). The financial support of Ministry of Education of Finland through the National Graduate School in Engineering Mechanics is gratefully acknowledged.

It has been an honour to have Professor Josef Eberhardsteiner from The Vienna University of Technology and Stefania Fortino from VTT as the preliminary examiners of this thesis.

I want to express my gratitude to supervisor Professor Jukka Tuhkuri for his encouraging words when needed most. Also, I would like to thank my advisor Jouni Freund for his guidance during my work and our valuable discussions. In addition, I am very grateful to my colleague Alp Karakoç for all of his help during the process. I would also like to thank everyone in working in the Department of Applied Mechanics. A special thanks goes to Susanna Hurme, Pasi Lindroth, Anssi Karttunen, Eeva Mikkola and Halid Yıldırım for our valuable coffee break discussions.

I am very thankful for my parents for their encouragement. My siblings, their families and my friends are all acknowledged for their support. Finally I want to thank my husband Ville, who has been there for me for the whole duration of the thesis process.

Espoo, March 17, 2015,

Johanna Sjölund

Contents

List of Publications

This thesis consists of an overview and of the following publications which are referred to in the text by their Roman numerals.

I J. Sjölund, A. Karakoç, J. Freund. A new approach for determining the hidden material parameters of a honeycomb. *Journal of Materials Science*, 49, 14, p. 4998–5005, April 2014.

II J. Sjölund, A. Karakoç, J. Freund. Accuracy of regular wood cell structure model. *Mechanics of Materials*, 76, p. 35–44, September 2014.

III J. Freund, A. Karakoç, J. Sjölund. Computational homogenization of regular cellular material according to classical elasticity. *Mechanics of Materials*, 78, p.56–65, November 2014.

IV J. Sjölund, A. Karakoç, J. Freund. Effect of cell geometry and material properties on wood rigidity. Accepted for publication in *International Journal of Solids and Structures*, February 2015.

Author's Contribution

Publication I: "A new approach for determining the hidden material parameters of a honeycomb"

The paper presents a method for finding the hidden parameters of a honeycomb structure by comparing physical experiments and simulations. The author wrote the manuscript, performed the physical experiments of one cell size and analysed the images to find the statistical data of the geometry.

Publication II: "Accuracy of regular wood cell structure model"

The paper presents a method for comparing the effect of different geometric and material parameters on the effective rigidity of a regular material. Spruce earlywood was considered as a case study. The author wrote the manuscript, performed the statistical analysis of the geometry and calculated the error measures.

Publication III: "Computational homogenization of regular cellular material according to classical elasticity"

The paper presents a two-scale computational homogenization method for deriving the effective elastic parameters of regular cell material. The author contributed to writing the article and used the developed method for spruce case study.

Publication IV: "Effect of cell geometry and material properties on wood rigidity"

The paper presents a method for finding the effect of different geometric and material parameters on the effective rigidity of wood. Spruce was considered as a case study. The author wrote the manuscript, analysed the geometry, performed the simulations and analysed the results.

Nomenclature

Symbol	Description
A	Area of polygonal domain / cell
A_b	Cross-sectional area of beam
b	Constant
$\vec{c}^n$	Translation vector
$\mathbf{C}, C_{ijkl}$	Compliance coefficient
C^0_{ijkl}	Effective compliance coefficient
D_{ijkl}	Rigidity coefficient
e	Sensitivity measure
$\hat{e}_i$	Basis
E	Exterior vertex points
E_s	Young's modulus of cell wall
E_i	Elastic moduli
E_{ijkl}	Fourth order elasticity dyad
E^0_{ijkl}	Effective elasticity dyad
$\vec{f}$	External load
$\mathbf{f}$	Compliance expression
$\vec{F}$	Stress resultant
$\underline{\vec{F}}_i$	Force acting on point i
$\vec{g}$	Relative position expression
G_{ij}	Shear modulus
G^0_{ij}	Effective shear modulus
h	Cell wall height
h_{lit}	Cell wall height, literature case
$\overset{\leftrightarrow}{H}, \mathbf{H}, H_{ij}$	Stretch
$\vec{i}, \vec{k}, \vec{k}$	Basis vectors
$\vec{i}^e, \vec{j}^e, \vec{k}^e$	Basis vectors of the cell wall coordinate system
I	Second moment of area

I_b	Second moment of area of the beam
$\mathbf{I}, I_{ijkl}$	Unit dyad
I_{ext}	Exterior points of the polygonal domain
$\underline{k}$	Measured spring constant
k_i, k	Modelled spring constant
$\mathbf{K}_{ij}$	Stiffness matrix
$\vec{l}_i$	Position of point i
l_{lit}	Cell wall length, literature case
l_N	Cell structure length
$\vec{m}$	External load
$\vec{M}$	Stress resultant
$\underline{\vec{M}}_i$	Moment at point i
n_u	Specimen size
pdf	Probability density function
P	External load
$\mathbf{q}_i$	Generalized displacement
r	Location in the growth ring
$\vec{r}$	Position vector
$\vec{r}^n, \vec{r}^{nm}$	Position vector of the vertex point
$\vec{r}_i$	Position vector of point i
$\mathbf{R}, R_{ij}$	Rotation dyad
si	Specimen number
$\vec{S}_i$	Directed length of point i
t	Cell wall thickness
t_e	Earlywood cell wall thickness
T	Depth of the cell
u_i	Displacement vector
$\vec{u}_0$	Displacement vector of a vertex point belonging to the boundary extreme
$\vec{u}_i$	Displacement of vertex point i
u_i^0	Rigid body displacement
Δu_i	Remainder displacement
$\mathbf{U}, U_{ij}$	Stretch dyad
V^0	Volume of a representative cell
w	Cell width
w_e	Earlywood cell width
w_N	Cell structure width
δW	Virtual work expression

δW^e	Virtual work expression of a cell wall
δW^{ext}	External virtual work expression
δW^{int}	Internal virtual work expression
δW^0	Effective virtual work expression
α, β,γ	Dimensionless quantities of geometry
α_s	Slenderness ratio
β_{lit}	Rigid body rotation, literature case
ϵ_{ijk}	Permutation symbol
ε_{ij}	Strain
ε_{ij}^0	Effective strain
ε_{ij}^*	Shape parameter
$\Delta\varepsilon_{ij}$	Remainder strain
ζ	Translation direction
θ	Rotation angle
$\vec{\theta}_i$	Rotation of a vertex point i
θ_i^0	Rigid body rotation
κ	Parameter of the distribution
λ	Parameter of the distribution
$\mu(a)$	Mean value of a
$\overset{\leftrightarrow}{\mu}$	Couple stress
ν_{ij}	Poisson's ratio
Ξ	Material parameters
Π	Function to be minimized
$\vec{\rho}, \vec{\rho}^{\,n}, \rho_i$	Relative position
$\vec{\rho}_0(i)$	Reference structural element
$\vec{\rho}^{\,m}$	Translation direction
$\sigma(a)$	Standard deviation of a
$\sigma_{ij}, \overset{\leftrightarrow}{\sigma}$	Stress
σ_{ij}^0	Effective stress
Υ	Geometric parameters
ϕ_{lit}	Angle of the structural element, literature case
$\overset{\leftrightarrow}{\phi}, \vec{\phi}, \phi_i$	Micro-rotation
φ	Material orientation

1. Introduction

Cellular materials, such as sandwich panels and wood (Gibson & Ashby 1997) are commonly used in engineering applications, where a good combination of rigidity and weight are needed. The applications range from construction to pulping and scales from hundreds of meters to parts of a millimetre.

The elastic properties of cellular materials need to be known for efficient use in the engineering applications. Making a reliable estimation of rigidity based purely on physical experiments requires a large number of experiments due to statistical description required (material properties vary), and dependency on the measuring scale. Simulation experiments give freedom of design so that scale, different features and their effect can be studied separately.

Cell structure rigidity depends on multiple geometric and elastic features. The geometric features include the geometry of the structure and the thickness of the cell walls. The elastic features include the elastic parameters of a cell wall. The descriptions can be either statistical or deterministic and include more and more parameters as the cell structure becomes more complex.

Simulation on a cellular structure requires knowledge not only on the effect of the important features but also of the features that are left out. Knowing the effect it is possible to have an estimation on the error caused by the simplifications used.

According to review by Mishnaevsky & Qing (2008) most micromechanical models of wood are based on a cell structure, where a hexagonal cell is repeated in a more or less regular manner (Gibson & Ashby 1997, Zienkiewich & Taylor 2002). The method ignores completely the statistical nature of the geometric and material parameters. The study by Fazekas et al. (2002) describes an irregular cellular structure by a Voronoi diagram. Although this does contain the effect of geometric irregularity, the Voronoi triangulation does not recognize some geometric features, such as elongated cells, that have an effect on the rigidity of the structure. A few references consider the irregularity of wood by tracing the scanned image on a cell-by-cell basis (Persson 2000, Holmberg et al. 1999, Kahle & Woodhouse 1994, Rafsanjani et al. 2012). Many of the studies consider only earlywood (Gibson & Ashby 1997, Watanabe et al. 2002). According to the reviews by Mishnaevsky & Qing (2008) and Hofstetter & Gamstedt (2009) also different scales up to the growth ring are important to include when modeling. The existing studies have different values for different parameters as well, for example the material parameters of a cell wall (Persson 2000, Jäger et al. 2011, Harrington et al. 1998, Sedighi-Gilani & Navi 2007).

1.1 Objectives and scope

The aim of the present work was to quantify the effect of the cell structure geometry and cell wall properties on the effective rigidity of Nomex and spruce materials. To add on the existing methods in literature the following steps were taken

- Geometric model is developed for a description of a cell structure which is used to generate statistically equivalent geometry.

- Computational homogenization method is adapted for cell structures to find the compliance of non-regular and regular cell structures. A new method is developed based on a particle model as the micromechanical model.

- A preliminary study on a simplified model of wood, in this case Nomex, is conducted. Beam model for the cell walls is validated by comparing the physical and simulated results of two different Nomex structures.

- A statistical description and a beam model for the cell walls are used to study the sensitivity of rigidity to variation in earlywood. A method was developed for calculating the effective rigidity for any combination of the geometric and cell wall parameters. The outcome is illustrated for selected parameters.

1.2 Dissertation structure

This thesis consist of a summary and four original research articles focusing on the analysing and modelling cellular structures in different scales. First in the summary a method for finding and analysing the geometry of a cellular structure is presented (Publications I and II). Statistical simulation of rigidity based on beams is presented (Publications I and II). A computational homogenization method applied to a regular geometry is developed (Publications III and IV). The statistical simulation is applied to Nomex, used here as a simplified model of wood, and the used beam model is validated by comparing the results of two different cellular structures (Publication I). For the statistical simulation only spruce earlywood is considered to find the effect of statistics on the rigidity (Publication III). Finally the homogenization method is applied to spruce earlywood and transition-/latewood to find the effective rigidity of spruce sample depending on the used geometric and elastic cell wall parameters (Publication IV).

2. Cellular structures

There exists many different types of cellular structures, both natural and man-made (Gibson & Ashby 1997). Unlike an idealized cell structure, most cellular structures have irregularities in their cell structure and material properties. These are obvious in natural materials, but also occur in manufactured cell structures. Irregularities have certainly effect on strength and may affect also rigidity (Zhu et al. 2001, Silva & Gibson 1995).

2.1 Connectivity and structural element

In this study, a structural element, which may be one cell, collection of cells or a part of a cell, is used as a basic building block for constructing a cellular structure. The structural element, defined by geometric parameters, is repeated and translated to form a cell structure. A regular structure is periodic and generated by repeating exactly the same structural element.

Regular structures are shown in Figures 2.1a, 2.1b, and 2.1c. For a non-regular structure some structural elements or parameters of the structural elements vary, examples of non-regular structures are shown in Figures 2.2a and 2.2b. An example of non-regular geometry with variation, where the parameters of the structural elements are statistical quantities is shown in Figure 2.2c.

The rigidity of a cellular structure may be contrary for different parameters of structural elements (Hohe et al. 1999). For example in Figure 2.1a and 2.1b the structural element is the same, only the parameters of the structural element are different. The hexagon has similar properties in all directions and the rectangle is very rigid in one direction and very flexible in the other.

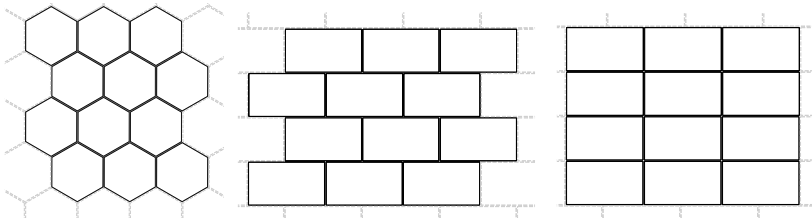

(a) Hexagonal **(b)** Overexpanded **(c)** Rectangular

Figure 2.1. Different regular cell structures, from left to right: hexagonal geometry, overexpanded hexagonal geometry with connectivity of three and rectangular geometry connectivity of four.

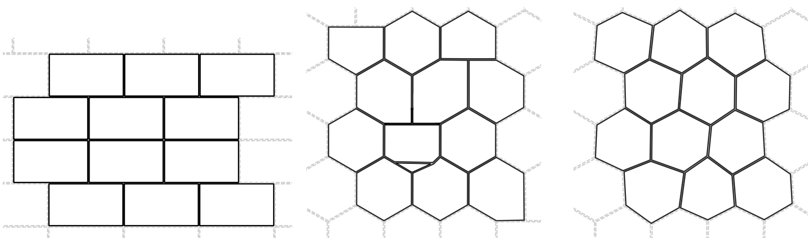

(a) Connectivity **(b)** Structural elements **(c)** Variation

Figure 2.2. Different non-regular cell structures, from left to right: varying connectivity, varying structural elements and variation in parameters.

For varying structural elements, shown in Figure 2.2b, not all structural elements are the same, but some cells may be hexagons, some cells triangles and some cells squares. Clearly, the whole geometry cannot be described with a one type of a structural element. Either many type of elements need to be used in the description, or one reference structural element, that describes the geometry with a desired accuracy, is selected.

The connectivity of a cell structure tells how the structural elements are connected to each other. Basically, it explains where the neighbours of a structural element are located. Connectivity has also an effect on the elastic properties of a cell structure. Examples of different connectivities are shown in Figures 2.1b and 2.1c, where in the first case the structure is very stiff in the vertical direction and in the second case the structure is very stiff in both the vertical and horizontal directions. Varying connectivity means that the neighbouring elements are connected in different ways. For example in Figure 2.2a, either three or four cell walls are connected to a vertex point.

2.2 Nomex

Structural sandwich panels with cellular core are widely used in, for example, aerospace and automotive applications, wherever high rigidity and low weight are required simultaneously (Karlsson & Aström 1997). The panels are composed of two skins separated by a lightweight core. Nomex cellular core, an example is shown in Figure 2.3, is made of aramid fiber paper (DUPONT Nomex or equivalent) coated with heat resistant phenolic resin. A sheet of the material is manufactured by connecting strips of paper to form a hexagonal structure.

Due to the fabrication method, the structure has double thickness ($2t$) and single thickness (t) walls. In Figure 2.3 the double thickness walls are vertical and all other walls have single thickness.

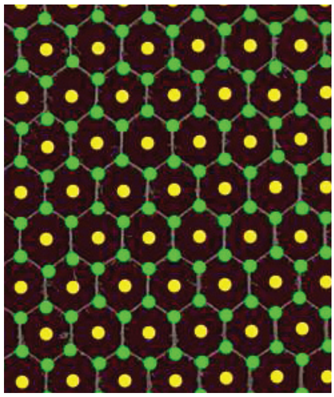

Figure 2.3. Nomex cellular structure. Double walls are vertically aligned. Cell centroids in yellow and vertex/corner points in green colour.

2.3 Softwood

Wood is an abundant, moderately durable and economically feasible natural product. It is widely used in construction, furniture, paper and pulping, printing and packaging industries. Material and geometric features of the cell and growth ring structures have significant roles when considering the rigidity of wood (Gibson & Ashby 1997). According to the reviews Mishnaevsky & Qing (2008), Hofstetter & Gamstedt (2009) different scales up to the growth ring affect the rigidity.

There are structural differences between softwoods and hardwoods. For example, rays in softwoods are more narrow and shorter than in hardwood. In softwoods the sap channels, apparent as very large cells, make

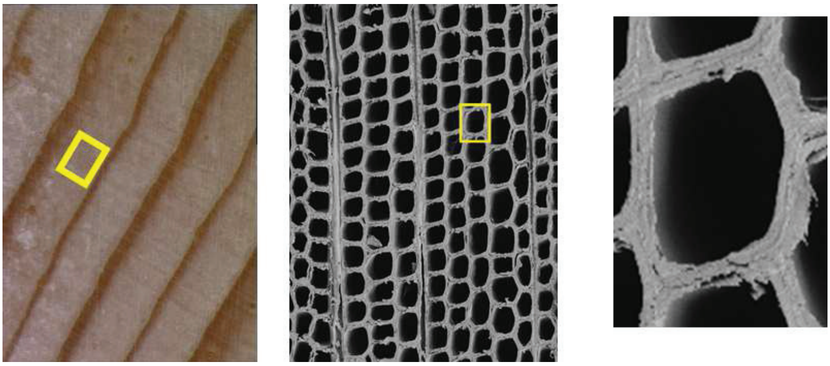

Figure 2.4. Different scales of wood. From left to right, growth ring scale, cell structure scale and cell scale.

up less than 3% of wood volume while in hardwood they can account for as much as 55%. Growth rings are also different in hardwoods and softwoods. Softwood growth rings consist of alternating circumferential bands of thick and thin walled cells. In hardwood growth rings are formed by bands of sap channels having large diameters and small diameters. Norway spruce was selected for this study because in wood industry plywoods and pulpwood are made with softwood species as spruce, it is one of the most common wood species in Finland, and softwoods have a more regular structure than hardwoods (Gibson & Ashby 1997, Bergman et al. 2010, Hugh 1976).

When considering wood, there exists features in multiple scales from cell wall level up to the whole trunk as shown in Figure 2.4. In each of the scales there are different features that have an effect on the rigidity of the next scale. The largest growth ring scale shows how wood grows differently during spring and summer, forming growth rings consisting of earlywood, transitionwood and latewood. In the beginning of year cells are larger and become smaller as the year goes round and at the same time also the cell walls become thicker. In the cell structure scale not all wood cells are alike, but there are deviations in size and shape. The wood cells are also longer in the transverse direction than in the radial direction and form lines in the transverse direction.

Wood cell walls have a microstructure containing layers and fibres, which makes the cell wall anisotropic and strong in the longitudinal direction (Gibson & Ashby 1997). The orthotropic nature of the cell wall is not taken into account if wood cell walls are modeled as beams as in Publication II.

3. Geometric model

The geometric model of the cell structure based on a structural element and translation mapping can be written as

$$\vec{r}^{nm} = \vec{c}^{m} + \vec{\rho}^{n} \tag{3.1}$$

in which superscript n identifies the vector belonging to the structural element, superscript m identifies the structural element, $\vec{c}^{m}$ is the translation vector of the structural element, and $\vec{\rho}^{n}$ is the relative position vector of the vertex points.

The model can be used to generate any regular structure, for example the structures shown in Figure 2.1. The specimen domain is required to fill completely, which limits the selection of the structural element and determines the translations accordingly.

3.1 Mapping model

In the mapping model the relative position vector of Equation (3.1) is given by

$$\vec{\rho}^{n} = \vec{\rho}_0(n) \cdot \overset{\leftrightarrow}{H} \tag{3.2}$$

in which $\vec{\rho}$ is the relative position vector of the reference structural element, $\overset{\leftrightarrow}{H}$ is the mapping which does not depend on n. The mapping model is illustrated in Figure 3.1.

To make the parameters of the mapping more physical, the rotation and deformation parts of H_{ij} can be separated by applying a polar decomposition

$$H_{ij} = R_{ik} U_{kj} \tag{3.3}$$

in which R_{ik} describes the rotation and U_{kj} describes the stretch and Einstein summation convention is used for the repeated subscript indices,

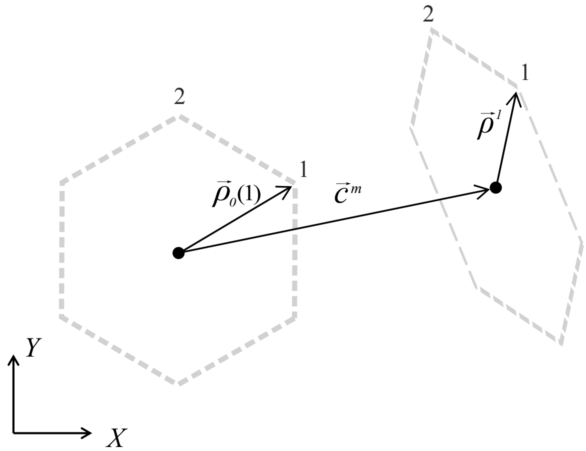

Figure 3.1. The mapping model, the reference structural element $\vec{\rho}_0(1)$, the translation $\vec{c}^m$ and relative position vector $\vec{\rho}^1$.

which means that the repeated indices are implicitly summed over. The parametrized matrix form of the rotation can be written as

$$\mathbf{R} = \begin{bmatrix} \cos\theta & -\sin\theta \\ \sin\theta & \cos\theta \end{bmatrix} \tag{3.4}$$

and the parametrized matrix form of the stretch as

$$\mathbf{U} = \begin{bmatrix} 1+\varepsilon^*_{xx} & \varepsilon^*_{xy} \\ \varepsilon^*_{xy} & 1+\varepsilon^*_{yy} \end{bmatrix}. \tag{3.5}$$

Parameter θ describes the orientation and ε^*_{xx}, ε^*_{xy}, and ε^*_{yy} the size and shape differences relative to the reference structural unit. The parameters are chosen such that their effect on the cell geometry is predictable.

Problem with applying the mapping model is that the same result may be achieved with multiple different mappings. Especially with regular hexagons, there exist symmetry every $\pi/6$ and the model cannot tell the difference between these angles. Also, the mapping model does not recognize certain geometric features as the number of parameters is only four. For these purposes a more general method was developed for wood.

3.2 Parameter model

In the parameter model, the relative position vector of Equation (3.1) is given by

$$\vec{\rho}^n = \vec{g}(n, ...) \tag{3.6}$$

in which n identifies the vertex point of the structural element and the dots stand for a list of geometric parameters defining the shape and size.

Unlike for the mapping model, the parametrization is chosen specifically for each case and defines the structural element directly.

3.3 Structural element

The structural element and the model should capture the important features in spruce and Nomex and also allow for asymmetry without being too complex. The element, used to produce the hexagonal cell collection via translation mapping, consists of three relative position vectors $\vec{\rho}(1)$, $\vec{\rho}(2)$, and $\vec{\rho}(3)$, around one translation point or vertex point (shown on the left in Figure 3.2). Since each vector has two components in the planar case, the description of the geometry contains nine parameters including the three cell wall thicknesses.

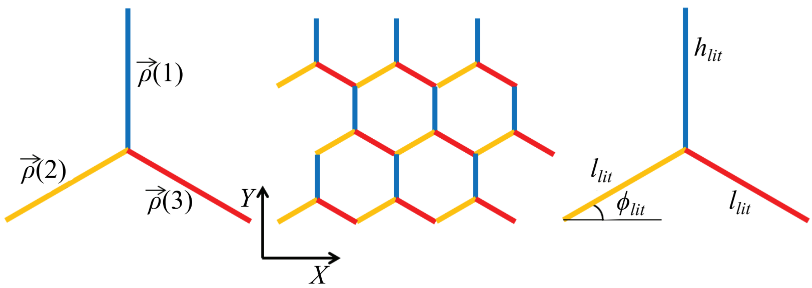

Figure 3.2. Structural element of the model on the left, the generated cell collection in the middle and a simplified model derived from the literature on the right. The rigid body rotation, β_{lit}, of the whole element is not shown.

A simplification of the model, referred to here as the literature case, represents the common choice discussed by, for example Gibson & Ashby (1997) is shown on the left in Figure 3.2. The problem with the simplified representation is its inability to represent asymmetric cells, even though asymmetry is known to have a large effect on rigidity (Watanabe et al. 2002). The detailed equations for calculating the parameters of the literature case from the three vector parameters are given in Publication II.

Another selection for the parameters is illustrated on the right in Figure 3.3. In this model, the cross-sectional parameters are limited to five: width, w, cell wall height h and the dimensionless quantities α, β and γ. The rotation of the whole structural element is not included. The thickness of the single cell wall t and depth of the cell, T, in the longitudinal direction are also needed to form a complete geometric description of the

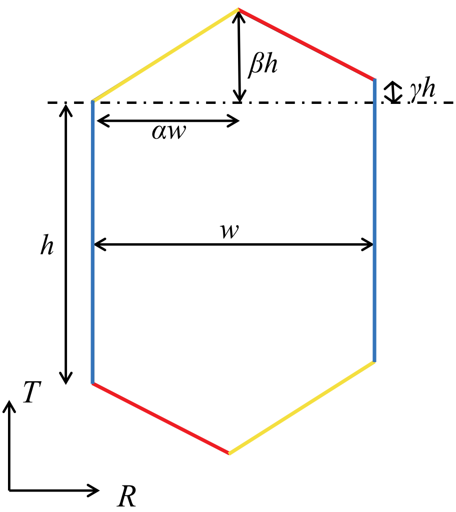

Figure 3.3. The geometric parameters of the cross section of the cell outer boundary geometry.

representative cell. These can be calculated from the parameters of the structural unit shown in Figure 3.2.

3.4 Parameter estimation

To find the parameters of the geometry, a collection of structural elements, for example in the middle of Figure 3.2, based on a specimen of Nomex and spruce are analysed. In the case of Nomex, the mapping model is utilized to find the parameters ε^*_{ij} and θ by mapping all structural elements back to a fixed reference structural element. For wood the parameters are the six coordinates of the relative position vectors.

As in the conventional pattern recognition studies by Chung et al. (2010), Bovik (2005), the separate cell regions are defined and their cell centroids are determined. Cell vertices or translation points, shown as white points in Figure 3.4 for spruce and as green points in Figure 2.3 for Nomex, are detected as the intersections of the adjacent cells that are sorted based on the nearest neighbour classification (Narendra & Fukunaga 1977, Khedr & Salim 2008). The cell wall thickness t is obtained as the distance between a vertex point and its nearest white pixel.

The geometry extracted as explained above can be used as the image geometry. Problem with these specimens is the limited number of cells and thus only limited scales can be studied using directly the extracted

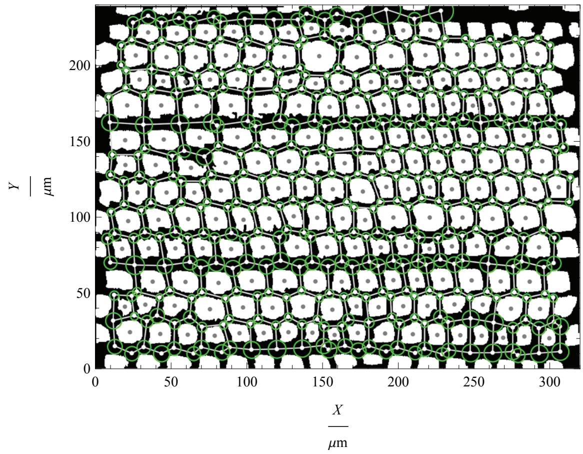

Figure 3.4. The corner points and circles with radius of cell wall thickness (green circles) for an earlywood specimen.

geometry. The image data can be processed further to find a more compact and general description of the geometry. The structural elements of the analysis are found from an image of the actual Nomex or Norway spruce.

Only the structural elements meeting the requirement of connectivity are included, so that three and only three differently coloured walls are connected to one vertex point as shown in Figure 3.2. For Nomex all structural elements filled the requirement. Depending on the image, approximately 10-20% of the cell walls were neglected for spruce earlywood and the results varied by a few percentage points depending on how the selection was made. The selection is illustrated for a case in Figure 3.5.

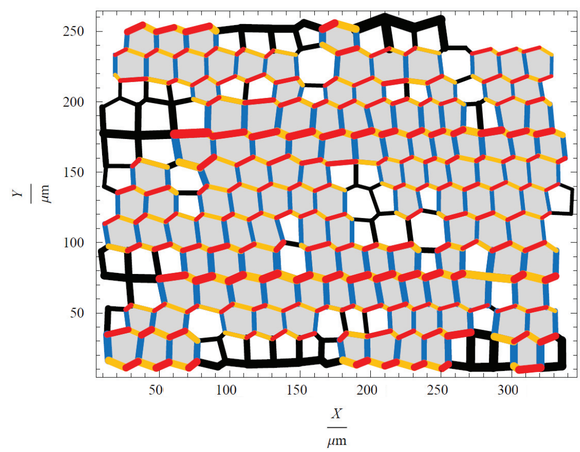

Figure 3.5. The set of structural elements that meet the requirement of connectivity of three and only three different coloured walls.

The found collection of values of structural elements can be used directly as the input for generating the geometry, but a distribution is utilized in order to find a statistical representation. To avoid the negative values and match the collection of values a log-normal distribution is used

$$\mathrm{pdf}(a) = \frac{1}{a\sqrt{2\pi\kappa}} \exp^{\frac{\ln a - \lambda^2}{2\kappa^2}}, \tag{3.7}$$

in which pdf is the probability density function, κ and λ can be expressed in terms of the mean value and standard deviation of data a. Then the variation in the cell scale is included by considering the parameters of the geometry as statistical quantities, which are defined by the mean value and standard deviation of each parameter. If the variation is small within a specimen, it can be assumed regular and described only by a single structural element.

The statistical variation is included in a geometry by first considering a regular structure and the variation is used to move the vertex points accordingly. When used repeatedly, with random values of the parameters from their distributions, the mapping creates slightly different geometries that are identical in statistical sense.

3.5 Discussion

The geometrical models gave a compact description that included the variation of the geometry and the asymmetry of the cells. On the other hand, the size and quality of the specimens was very limited and the method ignored some features, such as rays. Also, the method did not take into account the cell walls that did not meet the required connectivity.

4. Simulation experiment on rigidity

A simulation experiment on strength or rigidity has design like a physical one where a specimen is subjected to stress loading and the corresponding strain is obtained by direct measurement. In rigidity simulation the specimen is a collection of cells which is subjected to stress loading on the specimen edges as shown in Figure 4.1. A set of equilibrium stress loadings are used to calculate the corresponding strains to find the compliance of the material.

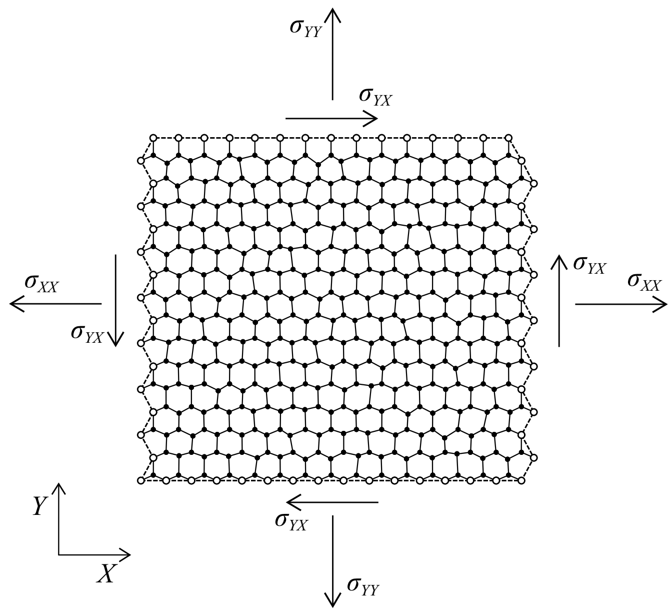

Figure 4.1. Specimen of cellular structure subjected to stress. Exterior points are marked with hollow circles, interior points with black circles, and polygon domain occupied by the specimen with a dashed line.

The compliance is obtained as a relationship between the strain ε_{ij} of the cell collection and the stress σ_{ij} acting on the specimen. The relationship between the strain and stress components can be written with the Einstein summation convention for linearly elastic material model as follows:

$$\varepsilon_{ij} = C_{ijkl}\sigma_{lk}, \tag{4.1}$$

in which $i, j, k, l \in \{X, Y, Z\}$ and the compliance C_{ijkl} characterizes material. Assuming that the XYZ-coordinate system is also the orthotropy coordinate system, the constitutive equation in terms of material parameters: Young's moduli E, Poisson's ratios ν, and the shear moduli G can be written in Voigt notation as

$$\begin{Bmatrix} \varepsilon_{XX} \\ \varepsilon_{YY} \\ \varepsilon_{ZZ} \\ 2\varepsilon_{YZ} \\ 2\varepsilon_{ZX} \\ 2\varepsilon_{XY} \end{Bmatrix} = \begin{bmatrix} \frac{1}{E_X} & -\frac{\nu_{YX}}{E_Y} & -\frac{\nu_{ZX}}{E_Z} & 0 & 0 & 0 \\ -\frac{\nu_{XY}}{E_X} & \frac{1}{E_Y} & -\frac{\nu_{ZY}}{E_Z} & 0 & 0 & 0 \\ -\frac{\nu_{XZ}}{E_X} & -\frac{\nu_{YZ}}{E_Y} & \frac{1}{E_Z} & 0 & 0 & 0 \\ 0 & 0 & 0 & \frac{1}{G_{YZ}} & 0 & 0 \\ 0 & 0 & 0 & 0 & \frac{1}{G_{ZX}} & 0 \\ 0 & 0 & 0 & 0 & 0 & \frac{1}{G_{XY}} \end{bmatrix} \begin{Bmatrix} \sigma_{XX} \\ \sigma_{YY} \\ \sigma_{ZZ} \\ \sigma_{YZ} \\ \sigma_{ZX} \\ \sigma_{XY} \end{Bmatrix}, \tag{4.2}$$

in which the elements satisfy the well known symmetry relationships so that there are in total nine independent parameters.

4.1 Specimen geometry

The specimen of the simulation experiment is built out of the three wall structural element on the left of Figure 3.2 with the mapping in Equation (3.1). The specimen is defined by the exterior points $i \in I_{ext}$ having connectivity less than three, meaning that less than three cell walls connect to a vertex point. The exterior points are shown as hollow circles and polygon edges are shown as dashed lines in Figure 4.1. The position vectors of the exterior points $\vec{r}_i$ and outward directed lengths $\vec{S}_i$ associated with these points are the important geometric quantities.

Directed lengths $\vec{S}_i$ are defined as the mean value of the directed lengths of the edges of the polygonal domain having a vertex point $i \in I_{ext}$ in common. With this definition for the directed lengths the following equations can be written

$$\sum_{i \in I_{ext}} \vec{S}_i = 0, \tag{4.3}$$

$$\sum_{i \in I_{ext}} \vec{r}_i \vec{S}_i = A\overset{\leftrightarrow}{I}. \tag{4.4}$$

In the latter relationship, A is the area of the polygonal domain and $\overset{\leftrightarrow}{I}$ is the second-order unit dyad defined by conditions $\vec{a} \cdot \overset{\leftrightarrow}{I} = \overset{\leftrightarrow}{I} \cdot \vec{a} = \vec{a}\ \forall \vec{a}$. The geometric relationships described above and the particular definition of the directed lengths associated with the nodes are based on the Gauss theorem applied to a polygonal domain. Further explanation of this can be found in Publications II and III.

4.2 Compliance derivation

In the micromechanical model, the cell walls are considered as slender bodies so that the force-moment-displacement-rotation interaction between two vertices is described accurately enough by the Bernoulli beam theory. Simulation with beams is used to find the force and displacement dependency for a collection of cells, of which an example is shown in Figure 4.1. In the material xyz-coordinate system, the equilibrium equations of beam are

$$\vec{F}' + \underline{\vec{f}} = 0, \tag{4.5}$$

$$\vec{M}' + \vec{i} \times \vec{F} + \underline{\vec{m}} = 0, \tag{4.6}$$

where $\underline{\vec{f}}$ and $\underline{\vec{m}}$ are the external load vectors, and $\vec{F}$ and $\vec{M}$ are the stress resultants acting on a beam cross-section. The prime symbol in $\vec{F}'$ and $\vec{M}'$ is used to denote the derivative with respect to x. Assuming that the x-axis coincides with the neutral axis of the beam, the constitutive equations for beam stress resultants of a linearly elastic material are

$$\vec{F} = (E_s A_b \, u_x') \, \vec{i} - \left(E_s I_b \, u_y''' \right) \, \vec{j}, \tag{4.7}$$

$$\vec{M} = (E_s I_b \, u_y'') \, \vec{k}, \tag{4.8}$$

in which u_x, u_y are the displacement components in the directions of the x- and y-axes, and E_s is the cell wall elastic modulus. The geometric properties of the beam cross sections are $A_b = Tt$ and $I_b = Tt^3/12$ in which t is the cell wall (or beam) thickness and T is the depth of the cellular structure.

Solutions to Equations (4.7) and (4.8) give the relationship between displacements and rotations of the beam ends and the forces and moments acting on the beam ends. The contribution of cell wall e to the virtual work expression of the cell structure can be written as follows:

$$\delta W^e = - \begin{Bmatrix} \delta \mathbf{q}_1 \\ \delta \mathbf{q}_2 \end{Bmatrix}^T \begin{bmatrix} \mathbf{K}_{11} & \mathbf{K}_{12} \\ \mathbf{K}_{21} & \mathbf{K}_{22} \end{bmatrix} \begin{Bmatrix} \mathbf{q}_1 \\ \mathbf{q}_2 \end{Bmatrix}, \tag{4.9}$$

where the matrix depends on the material, cross-sectional properties, and length of the cell wall, an example is given per unit depth in Appendix A of Publication II. The generalized displacements of the beam ends, consisting of displacements and rotations in the material coordinate system, are

$$\mathbf{q}_i = \begin{Bmatrix} u_{xi} \\ u_{yi} \\ \theta_{zi} \end{Bmatrix} = \begin{Bmatrix} \vec{i}^e \cdot \vec{u}_i \\ \vec{j}^e \cdot \vec{u}_i \\ \vec{k}^e \cdot \vec{\theta}_i \end{Bmatrix}, \tag{4.10}$$

in which $\vec{i}^e$, $\vec{j}^e$ and $\vec{k}^e$ are the basis vectors of the material coordinate system of cell wall e and $\vec{u}_i$, and $\vec{\theta}_i$ are the displacement and rotation of a vertex point i. Virtual work expression of the cell structure,

$$\delta W = \delta W^{int} + \delta W^{ext} = \sum_{e \in E} \delta W^e + \sum_{i \in I_{ext}} \begin{Bmatrix} \delta \vec{u}_i \\ \delta \vec{\theta}_i \end{Bmatrix}^{\mathrm{T}} \cdot \begin{Bmatrix} \underline{\vec{F}}_i \\ \underline{\vec{M}}_i \end{Bmatrix}, \tag{4.11}$$

accounts for the interaction with the surrounding cells with forces $\underline{\vec{F}}_i$ and moments $\underline{\vec{M}}_i$ in the second term. The sum in the second term is over the exterior vertex points E that define the boundary of the specimen. The forces and moments acting on the exterior points are expressed as follows:

$$\begin{Bmatrix} \underline{\vec{F}}_i \\ \underline{\vec{M}}_i \end{Bmatrix} = \vec{S}_i \cdot \begin{Bmatrix} \overset{\leftrightarrow}{\sigma} \\ \overset{\leftrightarrow}{\mu} \end{Bmatrix} \tag{4.12}$$

in which $\overset{\leftrightarrow}{\sigma}$ and $\overset{\leftrightarrow}{\mu}$ are the given force stress and the couple stress, respectively (Eringen 1999).

To exclude rigid body motion, the displacements and rotations of the exterior points are taken to be

$$\begin{Bmatrix} \vec{u}_i \\ \vec{\theta}_i \end{Bmatrix} = \begin{Bmatrix} \vec{r}_i \cdot \overset{\leftrightarrow}{\varepsilon} \\ \vec{\phi} \end{Bmatrix} \quad i \in I_{ext}, \tag{4.13}$$

in which $\overset{\leftrightarrow}{\varepsilon}$ is the constant symmetric strain and $\vec{\phi}$ the constant microrotation. The couple stress does not affect the virtual work expression, as deduced from Equation (4.11) combined with Equations (4.3), (4.12) and the knowledge that $\vec{\phi}$ is constant.

The principle of virtual work gives the displacements and rotations of the vertex points, u_{Xi}, u_{Yi}, and θ_{Zi}, and the three independent strain components, ε_{XX}, ε_{YY}, and ε_{XY}, as functions of the three stress components, σ_{XX}, σ_{YY}, and σ_{XY}, of the planar case. The relationship between the strain and stress components can be written as follows:

$$\begin{Bmatrix} \varepsilon_{XX} \\ \varepsilon_{YY} \\ 2\varepsilon_{XY} \end{Bmatrix} = \begin{bmatrix} C_{11} & C_{12} & C_{13} \\ C_{21} & C_{22} & C_{23} \\ C_{31} & C_{32} & C_{33} \end{bmatrix} \begin{Bmatrix} \sigma_{XX} \\ \sigma_{YY} \\ \sigma_{XY} \end{Bmatrix}, \tag{4.14}$$

in which C_{ij} $i,j \in 1,2$ are the components of the compliance. If the material is orthotropic and the XY-coordinate system is also the orthotropy system, the compliance can also be written in terms of Young's moduli and Poisson's ratios as

$$\begin{Bmatrix} \varepsilon_{XX} \\ \varepsilon_{YY} \\ 2\varepsilon_{XY} \end{Bmatrix} = \begin{bmatrix} \frac{1}{E_X} & -\frac{\nu_{XY}}{E_Y} & 0 \\ -\frac{\nu_{YX}}{E_X} & \frac{1}{E_Y} & 0 \\ 0 & 0 & \frac{1}{G_{XY}} \end{bmatrix} \begin{Bmatrix} \sigma_{XX} \\ \sigma_{YY} \\ \sigma_{XY} \end{Bmatrix}. \tag{4.15}$$

4.3 Continuity

The generated statistical structure needs to be geometrically or mechanically continuous. To generate a statistically equivalent geometry the locations of vertex points are found as random picks from the distribution defined by Equation (3.7).

Geometrically continuous means that the neighbouring cell walls are connected at the same vertex point. In practice, connectivity is enforced by selecting a common point of the vertex points after generating the structural elements of the mapping. For Nomex, the common vertex point was selected as a single random value for the connected vertex point. This method does not necessarily preserve statistics but generates a continuous structure.

Mechanically continuous structure, used for earlywood, requires only that the neighbouring cell wall ends have the same displacements and rotation but can be located at different points. In practice this is achieved by generating the structural elements of the mapping and then enforcing the points of common vertices to have equal displacements and rotations. This method ignores the geometric connectivity, but retains connectivity in what we call mechanical sense. A similar method is used in literature for non-matching meshes in opposite sides of representative volume elements by connecting the displacement fields (Nguyen et al. 2012).

To validate the method, the rigidity statistics were calculated for a set of structural elements, which were then scrambled and the rigidity statistics were calculated again. As the rigidity statistics were found to match, it can be concluded that the order of the structural elements does not affect the outcome and mechanical connectivity is enough.

4.4 Discussion

If the geometric parameters or the cell wall properties are statistical quantities like in Figure 4.1, the compliance is also a statistical quantity. For a reliable estimation of the population characteristics like mean values and standard deviations of the effective elastic parameters, the experiment is repeated on a random sample from the population. The variation in a population depends on the population size, specimen size and on the variation of the geometric and cell wall parameters.

The interactions with the surrounding material are modeled so that the specimens of an non-regular structure deform in the same manner as they would as part of a infinite collection of cells. To achieve a geometrically repeating specimen, the statistical variation is restricted to the interior structural elements and the exterior structural elements are regular. If the requirement geometric connectivity of specimens would be relaxed to mechanical connectivity on the borders of a non-regular specimen, the effect of borders could be reduced. As mechanical connectivity does not require geometrical continuity, the borders could be modeled as non-regular as well.

5. Computational homogenization

Computational homogenization characterizes a collection of methods to calculate the effective elasticity of a regular cell structure. Homogenization methods have been discussed, for example by Nguyen et al. (2012), Gibson & Ashby (1997), Hohe & Becker (2000), Charalambakis (2010) and Hassani & Hinton (1998). These include for example surface averaging method, volume averaging method and two scale expansion. In this study, a two scale expansion method, similar to the one by Hohe & Becker (2000), is used.

Here the effective elasticity is calculated by matching the virtual work expressions of two models, precise micromechanical model and effective continuum model. The explained method is discussed in more detail in Publications III and IV. The precise model describes the behaviour of the collection of cells in a detailed manner and contains the geometry of the structure and cell wall mechanical properties. The effective model is the continuum model and assumes that the material is continuous and the material properties are constant in the specimen.

In what follows the structural element in the precise model is a cell modeled as long hollow prism built out of six cell walls. As the material is considered regular, the cell collection can be generated by translating and repeating a representative structural element.

5.1 Periodic elastic material

Again in what follows, Einstein summation convention is used and superscripts identify cells. The stress-strain relationship of linearly elastic material can be written in the form

$$\sigma_{ij} = E_{ijkl}\varepsilon_{lk}, \tag{5.1}$$

in which E_{ijkl} is the fourth order elasticity dyad, σ_{ij} is the second order symmetric stress tensor, and ε_{kl} is the second order symmetric strain tensor. Elasticity dyad of linearly elastic periodic material satisfies

$$E_{ijkl}(\vec{c}^n + \vec{\zeta}^m) = E_{ijkl}(\vec{\zeta}^m), \tag{5.2}$$

in which $E_{ijkl}(\vec{\zeta})$ is the elasticity dyad of the representative cell, $\vec{c}^n$ is the translation vector and $\vec{\zeta}^m$ is the translation direction. Translation vector $\vec{c}^n$ is a linear combination of $\vec{\zeta}^m$ with integer coefficients. The finite or infinite collection of cells can be thought to be built by translating and copying the representative cell, identified here by $n = 0$, as in mapping (3.1).

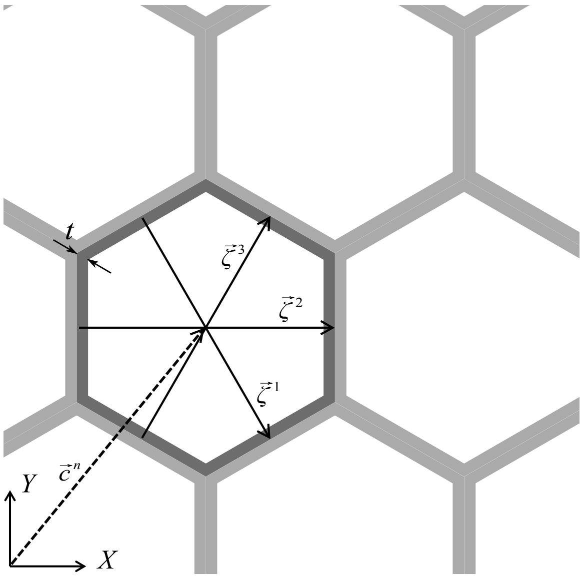

Figure 5.1. Cell wall thickness t, translation vector $\vec{c}^n$ and translation directions $\vec{\zeta}^1$, $\vec{\zeta}^2$, and $\vec{\zeta}^3$ of a representative cell as part of a cell collection.

5.2 Effective rigidity

In computational homogenization, the aim is to find the effective rigidity E^0_{ijkl} that describes the behaviour of an infinite collection of cells. The precise model is based on Equations (5.1) and (5.2). The counterpart for the precise model in Equation (5.1) can be written for the effective model as

$$\sigma^0_{ij} = E^0_{ijkl}\varepsilon^0_{lk} \tag{5.3}$$

in which σ^0_{ij} is the effective second order symmetric stress tensor, and ε^0_{lk} is the effective second order symmetric strain tensor.

In practice, the elastic properties of the effective model are chosen so that

$$\delta W - \delta W^0 = 0, \tag{5.4}$$

in which δW and δW^0 are the virtual work expression for the precise model and effective model, respectively. Virtual work expressions for the cells of the non-bounded collection are assumed to coincide so that it is enough to consider a representative cell only in Equation (5.4) under the periodicity assumption on displacement.

Precise model virtual work expression of Equation (5.1) is

$$\delta W = \int_{\Omega} (\delta\varepsilon_{ij}\sigma_{ij})\mathrm{d}V, \tag{5.5}$$

which corresponds to the classical elasticity theory without external distributed forces. Above, Ω is the domain occupied by the representative cell. Virtual work expression for the effective model is given by

$$\delta W^0 = \delta\varepsilon_{ij}^0\sigma_{ij}^0 V^0 \tag{5.6}$$

in which V^0 is the volume of the representative cell. One may think that the effective model strain ε_{ij}^0 is a constant approximation to precise model strain ε_{ij} and σ_{ij}^0 is that to σ_{ij} in the representative cell.

Displacements of the two models in a representative cell are related by

$$u_i = u_i^0 + \epsilon_{ijk}\theta_j^0\rho_k + \rho_j\varepsilon_{ji} + \Delta u_i \tag{5.7}$$

in which the first three terms on the right side of the equation represent the displacement of the effective model, ϵ_{ijk} is the permutation symbol, Δu_i is the remainder displacement by the precise model and translations u_i^0 and rotation θ_j^0 associated with the translation vector describe the small rigid body motion of the representative cell. The corresponding relationship for strains is

$$\varepsilon_{ij} = \varepsilon_{ij}^0 + \Delta\varepsilon_{ij}. \tag{5.8}$$

Due to the periodicity assumption of the solution, the remainder displacements Δu_i need to be continuous on the cell structure. Therefore the remainder displacement of the representative cell is subjected to

$$\Delta u_i(\vec{c}^0 + \frac{1}{2}\vec{\zeta}^m) = \Delta u_i(\vec{c}^0 - \frac{1}{2}\vec{\zeta}^m), \tag{5.9}$$

for all translation directions, see Figure 5.1.

5.3 Segregated solution method

In the variational problem for the effective elastic properties, Equation (5.4) is enforced for all variations of the effective strain and remainder displacement under the constraint in Equation (5.9). To be precise, the aim is to find the remainder displacement, Δu_i, and effective strain, ε^0_{ij}, such that

$$\int_\Omega (\delta\varepsilon^0_{ij}+\delta\Delta\varepsilon_{ij})E_{ijkl}(\varepsilon^0_{lk}+\Delta\varepsilon_{lk})\mathrm{d}V-\delta\varepsilon^0_{ij}\sigma^0_{ij}V^0=0 \quad \forall\delta\varepsilon^0_{ij} \text{ and } \forall\delta\Delta u_i. \tag{5.10}$$

To solve for the unknowns Δu_i and ε^0_{ij}, a two step segregated solution method is used. First, the effective strain is considered known, so that $\delta\varepsilon^0_{ij}=0$ and the variational problem in Equation (5.10) simplifies to finding the remainder displacement Δu_i that fulfills

$$\int_\Omega \delta\Delta\varepsilon_{ij}E_{ijkl}(\varepsilon^0_{lk}+\Delta\varepsilon_{lk})\mathrm{d}V=0 \quad \forall\delta\Delta u_i. \tag{5.11}$$

Since the equation is linear in ε^0_{lk}, solution to the strain due to the remainder displacement can be expressed as

$$\Delta\varepsilon_{ij}=D_{ijkl}\varepsilon^0_{lk}. \tag{5.12}$$

In the second step, the remainder displacement is considered as known, so that $\delta\Delta u_i=0$. As the outcome, the variational problem of Equation (5.10) simplifies to

$$\int_\Omega \delta\varepsilon^0_{ij}E_{ijkl}(\varepsilon^0_{lk}+\Delta\varepsilon_{lk})\mathrm{d}V-\delta\varepsilon^0_{ij}\sigma^0_{ij}V^0=0 \quad \forall\delta\varepsilon^0_{ij}. \tag{5.13}$$

As the effective strain ε^0_{ij} is constant in a representative element, the solution to the effective stress is given by

$$\sigma^0_{ij}=\frac{1}{V^0}\int_\Omega E_{ijmn}(I_{nmkl}+D_{nmkl})\mathrm{d}V\,\varepsilon^0_{lk}=E^0_{ijkl}\varepsilon^0_{lk} \tag{5.14}$$

in which I_{ijkl} are the components of the fourth order unit dyad and

$$E^0_{ijkl}=\frac{1}{V^0}\int_\Omega E_{ijmn}(I_{nmkl}+D_{nmkl})\mathrm{d}V \tag{5.15}$$

is the effective elasticity dyad. The effective compliance C^0_{ijkl} is the inverse of the effective dyad E^0_{ijkl} of Equation (5.15). A simple formula is obtained if D_{nmkl} is omitted in Equation (5.15). The upper bound for the stiffness obtained in this manner is simply the volume average of the precise model compliance.

5.4 Particle model homogenization

The homogenization method based on the precise and effective models allows one to choose the pair to be matched quite freely. The above method was based on a classical continuum model and linearly elastic material as the precise model, but a similar method can be used for a particle model based on forces and moments acting between the particles as the precise model.

Virtual work expression of the effective model is given in Equation (5.6) where $V = AT$, in which A is the area of the cell, chosen here as the structural element, and T is the depth of the cell. The virtual work expression of the precise model can be written as

$$\delta W = \sum_e \delta W^e, \tag{5.16}$$

in which sum extends over all the interacting particle pairs. The force-moment interaction of particles is modeled by considering the cell walls as slender Bernoulli beams. The expression of a single wall is given in Equation (4.9).

Here the relationship between the displacements of the two models, corresponding to Equation (5.7), takes the form

$$\begin{Bmatrix} u_i^\kappa \\ \theta_i^\kappa \end{Bmatrix} = \begin{Bmatrix} u_i^0 + r_j^\kappa \phi_j \\ \theta_i^0 \end{Bmatrix} + r_j^\kappa \begin{Bmatrix} \varepsilon_{ji} \\ 0 \end{Bmatrix} + \begin{Bmatrix} \Delta u_i^\kappa \\ \Delta \theta_i^\kappa \end{Bmatrix} \qquad \kappa \in I_{ext}, \tag{5.17}$$

in which ϕ_j is the constant micro-rotation. The expression is similar to Equation (5.12), but here both remainder displacement Δu_i^κ and remainder rotation $\Delta \theta_i^\kappa$ need to be included.

5.4.1 Case study of planar structures

Figure 5.2 shows eight planar cell structures. Markers of the exterior nodes indicate how the copies of structural elements are connected in a structure. Points with the same markers have the same displacements and rotations. Solid lines represent the cell walls; black line means that the wall belongs to one structural element and grey that the wall belongs to two structural elements when the structural elements are copied to form cell structures. In practice, depth $T/2$ of a beam in gray color is half of that indicated in black T, the cell walls are stacked on top of each other to have matching rotations and displacements at the beam ends.

The effective elastic parameter expressions are given in Table 5.1. The expression found for the equilateral triangle cell structure coincide with

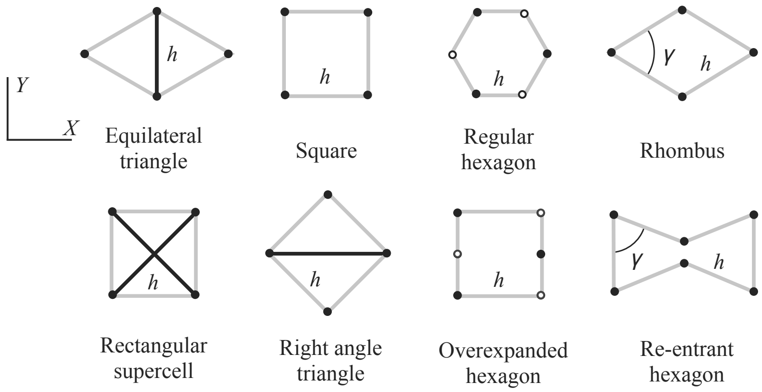

Figure 5.2. Cell type representative structural elements. Node connectivity is indicated by markers. Cell walls are in grey and black solid lines.

the ones reported by Wang & McDowell (2004), Gibson & Ashby (1997) and Gonella & Ruzzene (2008), although only the leading term in slenderness is accounted for. The square cell structure expressions match the ones by Wang & McDowell (2004). The expressions for the regular, over-expanded and re-entrant hexagon reported by Gibson & Ashby (1997) cell structures coincide as well.

Table 5.1. Parameters of classical elasticity as functions of slenderness $\alpha_s = t/h$. For lengthy expressions, only the leading term in α_s is given.

Cell	E_X/E_s	E_Y/E_s	ν_{XY}	ν_{YX}	G_{XY}/E_s
Equilateral triangle	$2\sqrt{3}\frac{\alpha_s+\alpha_s^3}{3+\alpha_s^2}$	$2\sqrt{3}\frac{\alpha_s+\alpha_s^3}{3+\alpha_s^2}$	$\frac{1-\alpha_s^2}{3+\alpha_s^2}$	$\frac{1-\alpha_s^2}{3+\alpha_s^2}$	$\frac{\sqrt{3}}{4}(\alpha_s+\alpha_s^3)$
Square	α_s	α_s	0	0	$\frac{1}{2}\alpha_s^3$
Regular hexagon	$\frac{4}{\sqrt{3}}\frac{\alpha_s^3}{1+3\alpha_s^2}$	$\frac{4}{\sqrt{3}}\frac{\alpha_s^3}{3+\alpha_s^2}$	$\frac{1-\alpha_s^2}{3+\alpha_s^2}$	$\frac{3-3\alpha_s^2}{1+3\alpha_s^2}$	$\frac{1}{\sqrt{3}}\frac{\alpha_s^3}{1+\alpha_s^2}$
Rhombus	$\frac{4\sqrt{3}\alpha_s^3}{1+3\alpha_s^2}$	$\frac{4}{\sqrt{3}}\frac{\alpha_s^3}{3+\alpha_s^2}$	$\frac{1-\alpha_s^2}{3+\alpha_s^2}$	$\frac{3-3\alpha_s^2}{1+3\alpha_s^2}$	$\frac{\sqrt{3}}{4}\alpha_s$
Rectangular supercell	$\sqrt{2}\alpha_s$	$\sqrt{2}\alpha_s$	$\sqrt{2}-1$	$\sqrt{2}-1$	$\frac{1}{\sqrt{2}}\alpha_s$
Right angle triangle	$\frac{\sqrt{2}\alpha_s}{1+2\sqrt{2}}$	$\sqrt{2}\alpha_s$	1	$\frac{1}{1+2\sqrt{2}}$	$\frac{1}{2}\alpha_s$
Overexpanded hexagon	$\frac{16\alpha_s^3}{1+16\alpha_s^2}$	α_s	0	0	$\frac{4\alpha_s^3}{5+\alpha_s^2}$
Re-entrant hexagon	$\frac{4\sqrt{3}\alpha_s^3}{1+3\alpha_s^2}$	$\frac{4\alpha_s^3}{3\sqrt{3}(1+\alpha_s^2}$	$\frac{-1+\alpha_s^2}{3+9\alpha_s^2}$	$\frac{-3+3\alpha_s^2}{1+3\alpha_s}$	$\frac{\sqrt{3}\alpha_s}{9+\alpha_s^2}$

5.5 Discussion

The discussed two-scale homogenization method applies to any regular structure and gives the effective rigidity of an infinite collection of cells with a single representative element. Any type of a cell wall model can be considered, for example the linearly-elastic material model or beam truss discussed earlier.

Comparison with literature of the eight cases (Wang & McDowell 2004, Gibson & Ashby 1997, Gonella & Ruzzene 2008) indicates that selection of the structural element of the cell structure does not affect the outcome as should be the case. The expressions of Table 5.1 assume that Young's modulus is the same for all the cell walls, thickness of the cell walls is constant and the cell geometry is described by just one parameter h. The expression become far more complicated for more complex cell structures as shown in Publication III.

The application based on the particle model and cell-type structural element gives a closed form expressions for the effective elastic parameters of a regular cell structure consisting of beams. The effect of the parameters is obvious from the closed form expressions. The drawback of the model is the assumption of regular cell structure that ignores all irregularities of the geometry and of cell wall parameters.

6. Rigidity of Nomex

Nomex honeycomb, of which an example is shown in Figure 2.3, is made of aramid material which is then coated with a phenolic resin. The relatively thin cell walls have single or double thickness because the material is fabricated by glueing strips of paper to form a cell structure.

An extensive literature survey on the theoretical and numerical studies on cellular cores or entire sandwich structures was conducted by Noor et al. (1996) and more recently by Hohe & Becker (2002). Schwingshackl et al. (2006) provided a quantitative evaluation of various available approaches for determining the properties of a cellular structure. In many papers on the sandwich core, the emphasis is on the out-of-plane direction (Meraghni et al. 1999, Foo et al. 2008). The in-plane properties are studied by for example Foo et al. (2007), Chen & Osaki (2009), and Chen (2010), but these studies consider only regular hexagonal cells. The studies by Karakoç & Freund (2012) and Karakoç et al. (2013) consider also non-regular cell structures.

Nomex is used as a simplified model of wood for which both physical and simulation experiments are possible. The aim is to validate the beam model for thin cell walls by comparing the physical and simulation results of two different cell geometries. The simplified model problem is used also to indicate how the cell wall properties can be estimated in cases where direct measurements are non-reliable and irregularities in the cell structure need to be taken into account.

6.1 Cell structure geometry

The Nomex material specimen, a part of which is shown in Figure 2.3, is analysed to find the geometric parameters ε^*_{xx}, ε^*_{xy}, ε^*_{yy}, and θ. The mapping model introduced in Section 3.1 is applied to a reference structural element, with $|\vec{\rho}_0(n)| = 1$ mm and in even angles. Specimens used in experiments are assumed to belong to the same population as they were cut from the same sheet of Nomex cellular structure.

The mean values and standard deviations of the geometric parameters are presented in Table 6.1. These describe the shape and size relative to the reference structural element. The mean value of the rotation angle describes the tilt of the whole specimen and so it is related to the position of the specimen during the scanning. The variation of θ describes the variation in the specimen and so is related to the population properties. The statistically equivalent geometry can be created by applying these parameters, for which an example is shown in Publication I.

Table 6.1. The mean value and standard deviation of the geometric parameters for cell size 6 mm.

	μ	σ
ε^*_{xx}	3.43	0.063
ε^*_{xy}	0.020	0.062
ε^*_{yy}	3.64	0.077
θ	0.51	0.016

Cell structure of Nomex material is relatively simple and variations of the geometric parameters were small, meaning that the variations could be ignored and the model could be simplified by a regular structure that uses only the mean values of the geometry.

6.2 Cell wall parameters

As the cell walls are relatively soft, thin and made of two materials, the cell wall thickness is difficult to measure accurately. Then also the Young's modulus cannot be easily determined by direct measurements as the tensile test and the flexural test may give different results for the Young's modulus.

To avoid the unreliable thickness measurement, the Young's modulus and thickness of a cell wall are calculated by an indirect manner minimizing the difference between the measured spring constant $\underline{k}$ from experiments and the spring constant k from simulations experiment. The experiment set-up is shown in Figure 6.1.

To find a combination of the Young's modulus and thickness of a cell wall, the best match between the simulation and physical experiment is

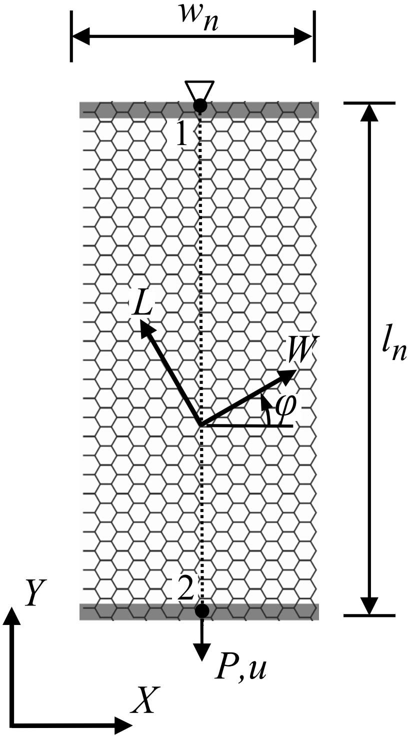

Figure 6.1. Schematic representation of the rigidity experiment.

calculated. In practice this can be achieved by minimizing the function

$$\Pi(E_s, t) = \sum_{\varphi} \sum_{i} (\underline{k}_{\varphi,i} - k_i(E_s, t, w_N, l_N, T, \varepsilon^*_{xx}, \varepsilon^*_{xy}, \varepsilon^*_{yy}, \varphi))^2, \tag{6.1}$$

in which i identifies the specimen number, φ is the material orientation angle between the material WL and laboratory XY-coordinate systems, and $\underline{k}$ is the measured spring constant of the cell material sample. The simulated spring constant k depends on the Young's modulus of a cell wall E_s, the thickness of a cell wall t, the shape parameters ε^*_{ij}, orientation φ, specimen width w_N, specimen length l_N, and core thickness T.

6.2.1 Physical experiments

Two samples of Nomex material, with nominal cell sizes 5 mm and 6 mm, are used in the experiments. The experiments are carried out on Nomex specimens in laboratory XY-coordinate system. The specimen is glued to aluminium profiles that are attached to the frame. The upper section of the specimen is pinned so that the line of action of P goes always through point 1 as shown in Figure 6.1. For a stiffness measure $\underline{k}$, a control point is chosen at the rigid body region and vertical displacement u_Y of this point is measured as a result of force P.

The independent variables of the rigidity experiment are φ, and the load magnitude P as illustrated in Figure 6.1. The dependent variable is the simulated spring constant k. Specimen size used in the experiments had the dimensions; width w_N =150 mm, specimen length l_N =300 mm, cell depth T = 12 mm.

Uni-axial tension tests are conducted for orientations $\varphi_1 = 0$, $\varphi_2 = \pi/6$, $\varphi_3 = \pi/3$ and $\varphi_4 = \pi/2$ relative to the laboratory coordinate system. Experiments are repeated three times in each orientation for the two different cell sizes 6 mm and 5 mm.

6.2.2 Simulation experiments

The simulation experiments are designed to match the physical experiments. The specimens are generated by applying the geometry found by geometric analysis and included the variation of the geometry. The thin cell walls are modeled as Bernoulli beams, which makes both the Young's modulus and thickness as cell wall properties.

Solutions to equations (4.5), (4.6), (4.7), and (4.8) for the beams are connected by continuity conditions for displacements and rotations at vertices and the equilibrium of the points 1 and 2 shown in Figure 6.1. The upper and lower boundary extremes (gray regions in Figure 6.1) are modeled as rigid bodies so that displacement is

$$\vec{u}_i = \vec{u}_0 + \vec{\alpha}_0 \times (\vec{l}_i - \vec{l}_0), \tag{6.2}$$

where $\vec{u}_i$ is the displacement vector, $\vec{\alpha}_0$ is the rotation vector, $\vec{l}_i$ is the position vector of a vertex point belonging to the boundary extreme, and $\vec{l}_0$ is the position vector for the translation point 1 or 2. For point 1 shown in Figure 6.1 $\vec{u}_0 = 0$ and $\vec{l}_0$ is the position vector of point 1. For point 2 $\vec{u}_0$ is the displacement vector of point 2 and $\vec{l}_0$ is the position vector of point 2. External forces and moments acting on the left and right boundary extremes vanish.

6.3 Results

The measured spring constants for different orientations in Table 6.2 are used to obtain the sets of the hidden parameters E_s and t as the minimizers of the equation (6.1). As expected the minimizer was not unique. The set of minimizers are illustrated in Figure 6.2 in the reasonable range t

$\in [0.05, 0.08]$ mm and $E_s \in [5, 15]$ GPa. These minimizers define a curve that can be expressed in terms of bending stiffness and thickness of the cellular structure as

$$\frac{E_s I}{T} = b, \tag{6.3}$$

in which $I = (Tt^3)/12$ and b is a constant, $b = 201$ Nm for cell size 6 mm and $b = 92$ Nm for cell size 5 mm.

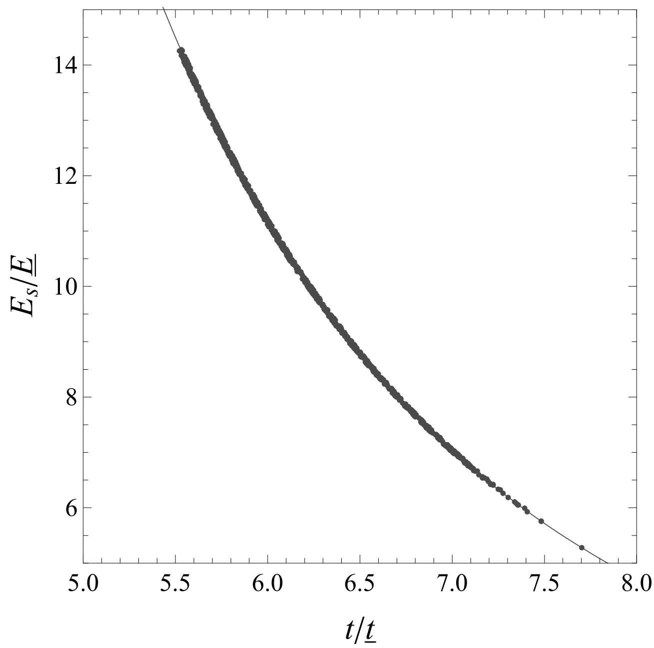

Figure 6.2. The relationship between E_s and t as a result of minimizing the Equation (6.1) for cell size 6 mm. Here, $\underline{t} = 10^{-5}$ m and $\underline{E} = 10^9$ Pa.

Table 6.2. The effective spring constants and their difference for different material orientations for cell size 6 mm.

	Physical exp.		Simulation exp.		$\frac{\lvert \underline{k}(\mu) - k(\mu) \rvert}{k(\mu)}$
	μ	σ	μ	σ	
$\varphi = 0$	805.4	89.2	913.6	0.3	12%
$\varphi = \pi/6$	1862.4	52.4	1653.4	0.9	13%
$\varphi = \pi/3$	1522.7	94.6	1619.9	1.1	6.0%
$\varphi = \pi/2$	922.6	36.7	957.9	0.4	3.7%

The spring constants of physical experiments and simulation experiments for different material orientations are presented in Table 6.2 for cell size 6 mm. Also given is the relative difference of the spring coefficients. The values of Young's modulus and thickness that gave the best match between physical and simulation experiments are used to obtain the simulated spring constants. The results show that the lowest and highest values of the spring constants were obtained for $\varphi = 0$ and $\varphi = \pi/6$, respectively. A larger difference was found between the measured and simulated spring constants at orientation $\varphi = 0$ and $\varphi = \pi/6$. For the orientations $\varphi = \pi/3$ and $\varphi = \pi/2$ the difference was smaller.

6.4 Discussion

Rigidity of Nomex material depends on geometric and elastic parameters, including the geometry, Young's modulus and the thickness of the cell wall as shown in Table 5.1 for hexagonal cell. The dependency is very strong e.g. with thickness, which means that accurate measurements are needed.

The model used for Nomex contained the variation of the geometric parameters. The effect was found to be relatively small as concluded from the standard deviations of the simulation experiments in Table 6.2. This means that the Nomex material could be assumed to be regular and the effective rigidity of a cell structure could be found for equilateral cellular sheet under regular hexagon in Table 5.1, when the elastic modulus is known.

The hidden parameter concept was introduced for cellular structure modeling. The method was used to match virtual and physical experiments to find the rigidity of Nomex cell wall material and thickness of a cell wall. Structural stiffness was used for finding the hidden parameters. As the minimizers of the difference between the spring constants of the physical and simulation experiments in the least square sense turn out to be non-unique representing the value for the bending stiffness of the material to be used for the cell walls.

The deviations between the physical experiments and the simulations can be caused by the measuring error, for example the specimen alignment on the test frame. In the analysis of the geometry, the walls are assumed to be straight and the vertex points are determined accordingly. This can cause some geometric modeling error in the simulations.

In order to validate the method, two different nominal cell sizes 6 mm and 5 mm were tested through physical and simulation experiments. The different sheets were made with the same material, but slightly different cell wall thicknesses. The Young's modulus is assumed to be the same for both cases, the depth is the same, the relation of the wall thicknesses of the two specimens was measured directly as $t_6/t_5 \approx 1,27$ and for the b values in Equation (6.3) $b_6/b_5 = (201/92)^{1/3} \approx 1,30$. The results are very close to each other which validates the used beam model.

7. Rigidity of spruce

Spruce has a complex structure with many details that all have an effect on rigidity. An example of cells, earlywood and growth ring structures is shown in Figure 2.4. Cell walls consist of a primary wall and a three layer secondary wall and two adjoining cell walls are connected by a middle lamella. The cell wall contains also structure strengthening fibres oriented in different directions (Bergman et al. 2010, Persson 2000).

A variety of models exist for wood, starting from very simple models and ending to models including tens of parameters. In the simplest model, wood is considered as equilateral regular cell structure (Gibson & Ashby 1997). However, it is found that also the shape of the wood cell has an effect on the anisotropy of the material (Kahle & Woodhouse 1994). In some models only earlywood is considered (Gibson & Ashby 1997, Watanabe et al. 2002). According to the reviews by Mishnaevsky & Qing (2008) and Hofstetter & Gamstedt (2009) also different scales up to the growth ring are important. In many of the studies earlywood and latewood are considered as separate and transitionwood is not included (Qing & Mishnaevsky Jr 2010, Qing & Mishnaevsky 2011, Koponen et al. 1991, Modén & Berglund 2008). A few studies include also the transitionwood (Wittel et al. 2005, Holmberg et al. 1999, Persson 2000, Bergander & Salmén 2000, Astley et al. 1998). The effect of microfibril angle, moisture or other parameters having an effect on the elastic properties of the cell wall have been considered by Jäger et al. (2011), Koponen et al. (1991).

The aim of the study is to find the relative effect of different geometric and material parameters on the rigidity, which gives insight into their importance. Finally, a simple model including only the most important parameters is developed that can be used to calculate the effective rigidity for any combination of the parameters. The effect of parameters on rigidity is illustrated by studying cell wall parameters, thickness and transition-/latewood separately.

7.1 Parameters of the model

The compliance and thus also the effective elastic parameters E_R, E_T, E_L, G_{RT}, G_{RL}, G_{TL}, ν_{RT}, ν_{LR}, and ν_{LT} depend on the elastic parameters of the cell wall material assumed orthotropic and geometric parameters of the cell structure as

$$\mathbf{C} = \mathbf{f}\left(\Xi, \Upsilon\right), \tag{7.1}$$

in which $\Xi = \{E_1, E_2, E_3, G_{12}, G_{13}, G_{23}, \nu_{12}, \nu_{31}, \nu_{32}\}$ are the cell wall parameters, $\Upsilon = \{t, \vec{\rho}(1), \vec{\rho}(2), \vec{\rho}(3), n_u\}$ are the geometric parameters, t is the thickness of a cell wall, $\vec{\rho}(1), \vec{\rho}(2), \vec{\rho}(3)$ define the structural element in Figure 3.2, and n_u is the size of the specimen. The geometric and elastic parameters are considered as statistical quantities described by their mean values and variations.

The effect of the parameters on the compliance, which is presented in (4.14) or (4.2), is quantified by the sensitivity measure

$$e = \frac{\parallel \mathbf{C} - \mathbf{C}_{ref} \parallel}{\parallel \mathbf{C}_{ref} \parallel}, \tag{7.2}$$

in which $\mathbf{C}$ is the compliance, $\mathbf{C}_{ref}$ is the reference compliance, and the Euclidean matrix norm is used (Boas 1983). As the geometric and material parameters are statistical quantities, $\mathbf{C}_{ref}$ and $\mathbf{C}$ are also statistical quantities described by the mean value, $\mu(e)$, and standard deviation, $\sigma(e)$.

Including all possible details or parameters would make a very complex model and require large computational effort. A parameter may however be omitted if the relative effect to rigidity is small.

7.2 Cell structure geometry

The coordinate systems, an example of earlywood cell, and a collection of cells are shown in Figure 7.1. The axes of the cell wall coordinate system are as follows: index 1 is the direction of the cell wall thickness, 2 is the direction of the cell wall length and 3 is the direction of the wall depth. The axes of the cell coordinate system are chosen to follow the commonly used notation in which R denotes radial direction, T denotes tangential direction and L denotes depth direction. Although RTL-coordinate system is actually curvilinear, the effect is omitted due to small size of the specimen relative to the radius of curvature of the growth ring.

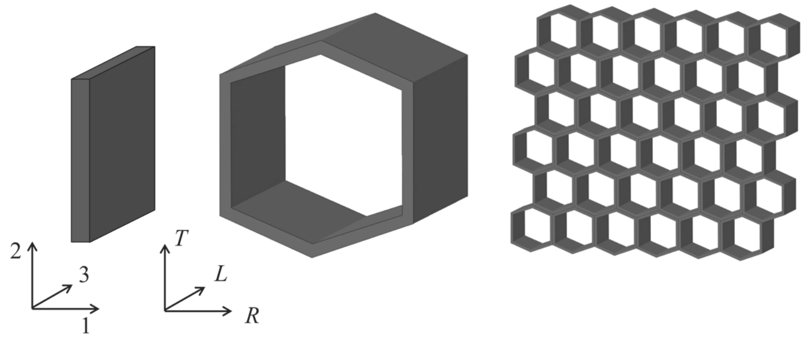

Figure 7.1. The orientations of the cell wall and cell coordinate systems. Left to right: wood cell wall, one wood cell and a specimen.

To find a statistical description of the geometry, ten specimens ($s1$–$s10$) of spruce earlywood are analysed with the method in Chapter 3. The wood specimens are from the same 60 year old Norway spruce stem grown in Finland. All specimens were cut from mature wood to avoid the changes in the cell geometry and microfibril angle during the first 10 growth rings (Sarèn et al. 2001). Specimen $s4$ is presented in Figure 3.4.

The structural element utilized in the analysis is shown on the left of Figure 3.2. The mean values and standard deviations of geometric parameters are given in Table 7.1 as components of $\vec{\rho}(1)$, $\vec{\rho}(2)$ and $\vec{\rho}(3)$. As the $\rho_X(1)$ mean values differed from zero, the image is slightly rotated and the XY-coordinate system of the analysis does not exactly match the commonly used RT-coordinates.

The mean values of the geometric parameters of Figure 3.3 as calculated from the mean values of Table 7.1 are given in Table 7.2. To calculate the mean values of the geometric parameters of the ten specimens, the results were rotated from the XY-coordinate system to the RT-coordinate system.

7.3 Cell wall parameters

The orthotropic cell wall material has nine parameters; the elastic moduli E_1, E_2, E_3, the shear moduli G_{12}, G_{13}, G_{23} and the major Poisson's ratios ν_{12}, ν_{31}, ν_{32}. The cell wall parameters vary in the specimen and from specimen to specimen. There also exist variation in the parameters found in the literature. The aim is to find the effective elastic parameters as

Table 7.1. The mean values and standard deviations of the structural element vectors and the thickness of the cell walls.

	[μm]	$\rho_X(1)$	$\rho_Y(1)$	$\rho_X(2)$	$\rho_Y(2)$	$\rho_X(3)$	$\rho_Y(3)$	$2t$
$s1$	μ	-1.80	16.6	-10.6	-4.24	11.4	-3.97	3.01
	σ	1.82	3.54	5.11	1.30	4.95	1.31	0.977
$s2$	μ	-0.498	16.6	-11.4	-4.03	9.66	-3.98	3.18
	σ	1.72	4.91	3.71	1.20	3.90	1.11	1.11
$s3$	μ	-1.13	15.0	-10.7	-4.78	10.7	-4.30	3.31
	σ	1.37	4.83	4.59	1.35	3.74	1.17	1.26
$s4$	μ	-1.11	16.1	-10.1	-4.04	10.7	-3.99	3.74
	σ	1.56	2.40	3.29	0.992	3.36	0.980	1.20
$s5$	μ	-0.159	16.2	-13.6	-5.04	12.1	-4.81	3.77
	σ	1.48	4.80	4.72	1.44	4.59	1.36	1.17
$s6$	μ	-0.740	16.3	-12.9	-5.25	12.0	-4.95	4.05
	σ	1.66	4.56	5.13	1.77	5.63	1.47	1.20
$s7$	μ	-0.155	18.4	-14.6	-4.81	12.8	-4.99	3.39
	σ	1.96	4.86	6.64	1.78	7.99	0.321	1.03
$s8$	μ	-0.738	20.8	-12.7	-4.97	11.6	-4.82	3.58
	σ	2.30	3.05	5.71	1.64	4.70	1.50	1.13
$s9$	μ	-0.421	17.7	-16.8	-5.19	11.5	-5.21	3.14
	σ	1.93	5.00	6.42	1.87	5.66	2.09	0.927
$s10$	μ	-2.01	17.6	-12.4	-5.08	12.9	-4.33	3.09
	σ	1.65	3.48	4.43	1.23	5.95	1.18	1.01

Table 7.2. The smallest and largest values or a single value of geometric parameters.

	Smallest	Largest
w	0.0234 mm	
h	0.0172 mm	
α	0.524	
β	0.241	
γ	0.056	
T	0.2 mm	
t	0.0007 mm	0.0027 mm

function of the cell wall parameters in the range found from the literature.

The smallest and largest values found from literature are given in Table 7.3 (Persson 2000, Jäger et al. 2011, Harrington et al. 1998, Sedighi-Gilani & Navi 2007). The elastic modulus E_3 is assumed constant as it is always significantly larger than E_1 and E_2, there is no variation in the cell in the depth direction, and the depth of the cells is clearly larger than width. The shear moduli are assumed to be related by $G_{13} = G_{23}/0.92$.

Table 7.3. The smallest and largest values of cell wall elastic parameters.

	Smallest	Largest
E_1/E_2	1	2
E_3/E_2	10	
G_{12}/E_2	0.25	0.65
G_{23}/E_2	0.3	0.5
G_{13}/E_2	0.33	0.54
ν_{12}	0	0.5
ν_{31}	0	0.5
ν_{32}	0	0.5

7.4 Sensitivity to parameter variation

The effect of geometric and cell wall material parameter variations and size of the specimen is quantified by comparing the compliances as given by six somewhat different models called here Reg (Regular), Lit (Literature), Ima (Image), Sta(t) (Statistical with respect to t), Sta($\vec{\rho}$) (Statistical with respect to $\vec{\rho}$), and Sta($\vec{\rho}, t$) (Statistical with respect to $\vec{\rho}$ and t). Planar beam model, based on considering only earlywood with relatively thin cell walls, is used for the cell walls in all cases so that the parameters of the compliance in Equation (7.1) reduce to $\Xi = \{E_s\}$, $\Upsilon = \{t, \vec{\rho}(1), \vec{\rho}(2), \vec{\rho}(3), n_u\}$. All parameters are considered statistical quantities defined by a mean value and a standard deviation which means that the compliance and the sensitivity measure are also statistical quantities.

Two different sizes are studied to see the effect of specimen size when modeling non-regular structures. The specimen sizes chosen for the simulations are $n_u = 15 \times 12$ and $n_u = 40 \times 40$ cells, referred to as the small and large size, respectively. The specimen size n_u affects the mean value of the compliance and especially the variation of the compliance.

The regular geometry (called Reg) based on the structural element shown on the left in Figure 3.2 and mean values given in Table 7.1 are used to calculate $\mathbf{C}_{ref}$ in the sensitivity measure e in Equation (7.2). The compliance of the regular structure using the mean values of the parameters is given in Appendix B of Publication II for a planar case.

The cases defining $\mathbf{C}$ of the sensitivity measure in Equation (7.2) are Lit, Ima, Sta(t), Sta($\vec{\rho}$), and Sta($\vec{\rho}, t$). The Lit case, for which geometry is shown on the right in Figure 3.2, is based on the mean values of the parameters and does not consider asymmetry. The compliance of Lit is calculated as in Chapter 5 for a planar case. The Ima case is based directly on the scanned image of spruce earlywood. The Ima case can only be studied in the small size as larger size images are not available. Sta($\vec{\rho}$) considers only variation of the geometry. Sta(t) considers only variation of the thickness. Sta($\vec{\rho}, t$) considers both variation of thickness and geometry together. The geometries of the non-regular structures (Ima and Sta) that include variation are modeled as in Chapter 3 and the compliances are calculated as in Chapter 4.

The sensitivity measures for the large size were given in Table 7.4 and for the small size in Table 7.5. The Lit case had relatively small sensitivity measures as asymmetry was not very large in the specimen. The effect of thickness variation Sta(t) was found to be significant, at most 99%. The effect of geometry variation Sta($\vec{\rho}$) was relatively small, at most 13%. Also, the effect of both the variation in the geometry and thickness Sta($\vec{\rho}, t$) was calculated; it was discovered that the total effect was smaller than with only the variation in the thickness. This was to be expected due to the fact that the dependencies of the compliance on the thickness and length of the cell wall were somewhat opposite. The Image case had large variation from specimen to specimen and was of the same magnitude as Sta(t). A more detailed explanation and the sensitivity measure where C_{ref} is for Ima case can be found in Publication II.

In addition to the cell wall thickness and geometry, the effect of variation in the Young's modulus is also studied. If a standard deviation of 20% was used for the Young's modulus of the cell wall, defining $\mathbf{C}$, the effect on the difference measure, e, was under 5%.

In what follows the statistical variation of parameters is omitted. It can be deduced that leaving out the geometry variation does not significantly affect the compliance but simplifies the calculations. The impact of the cell wall material and thickness parameter variation is clear when

Table 7.4. Mean value of the sensitivity measure e compared to the Reg case in terms of percentages for $n_u = 40 \times 40$.

	Lit	Sta(t)	Sta($\vec{\rho}$)	Sta($\vec{\rho}, t$)	Ima
$s1$	8.3%	73%	7.5%	56%	-
$s2$	6.4%	88%	11%	64%	-
$s3$	6.2%	99%	9.4%	72%	-
$s4$	6.3%	74%	3.5%	65%	-
$s5$	5.0%	78%	8.0%	58%	-
$s6$	6.5%	72%	6.2%	70%	-
$s7$	4.7%	70%	8.0%	50%	-
$s8$	2.9%	67%	5.4%	55%	-
$s9$	15%	64%	11%	43%	-
$s10$	8.8%	78%	6.3%	62%	-

Table 7.5. Mean value of the sensitivity measure e compared to Reg case in percentages for $n_u = 15 \times 12$.

	Lit	Sta(t)	Sta($\vec{\rho}$)	Sta($\vec{\rho}, t$)	Ima
$s1$	8.3%	56%	9.6%	40%	51%
$s2$	6.4%	68%	13%	47%	39%
$s3$	6.2%	63%	11%	45%	60%
$s4$	6.3%	59%	4.8%	51%	39%
$s5$	5.0%	62%	8.8%	46%	48%
$s6$	6.5%	58%	8.3%	41%	53%
$s7$	4.7%	69%	11%	35%	61%
$s8$	2.9%	52%	6.9%	40%	49%
$s9$	15%	50%	13%	30%	33%
$s10$	8.8%	60%	8.2%	45%	77%

considering Table 5.1, where effective elasticity is proportional to the first power of the cell wall parameter E_s and to the third power of the thickness t. The cell wall material parameter variation can then be safely omitted. Thickness variation is left out, as the effect of the variation can be taken into account by using a thickness that differs from the mean value. This takes into account that the compliance depends on the third power of the thickness and $\mu(t)^3 \leq \mu(t^3)$.

7.5 Sensitivity to parameter mean values

To further simplify the spruce rigidity model, the sensitivity of the compliance to the mean values of the cell wall material parameters is considered. There, the specimen of either earlywood or latewood and the homogenization method in Chapter 5 is used to find the effective rigidity of a regular specimen. The cell walls are modeled as orthotropic with parameter values as in Section 7.3, the geometry as a three dimensional cell in Figure 3.3 and the specimen follows the coordinate systems of Figure 7.1. This reduces the parameters of the compliance to $\Xi = \{E_1, E_2, G_{12}, G_{23}, \nu_{12}, \nu_{31}, \nu_{32}\}$ and $\Upsilon = (t, w, h, \alpha, \beta, \gamma, T)$. The specimen size n_u does not affect the results for the regular specimen.

To find the sensitivity measure of the effective rigidity on the cell wall parameters, the cell wall parameters are given smallest and largest values in Table 7.3, defining $\mathbf{C}_{ref}$ and $\mathbf{C}$, respectively. Then the sensitivity measure describes the change in the compliance for the applied range of values. All other parameters are given the mean values of Tables 7.2 and 7.3, excluding Poisson's ratios that are given value 0.3. The non-zero sensitivity measures calculated as in Equation (7.2) for the elastic parameters are given in Table 7.6.

Table 7.6. Sensitivity of the compliance to the cell wall elastic parameters.

	e
E_1/E_2	0.11
G_{12}/E_2	0.11
G_{23}/E_2	0.54
ν_{32}	0.0082
ν_{31}	0.0160
ν_{12}	0.0665

The effect of the Poisson's ratio was found to be fairly small at most around 7% for the large range of values. Based on this, the Poisson's ratios were given values 0.3 for all cases. For other cell wall elastic parameters the effect was found to be relatively large. This further simplifies the elastic parameters of Equation (7.1) to $\Xi = \{E_1, E_2, G_{12}, G_{23}\}$.

7.6 Rigidity of a regular specimen

Using the same homogenization method as in the previous section, the effective rigidity can be calculated for any combination of the set of parameters $\Xi = \{E_1, E_2, E_3, G_{12}, G_{23}, G_{23}, \nu_{12}, \nu_{31}, \nu_{32}\}$ and $\Upsilon = (t, w, h, \alpha, \beta, \gamma, T)$. As computations require a single cell, the results have only a mean value and are relatively easy to calculate.

7.6.1 Effect of cell wall elastic parameters

To illustrate the effect of the cell wall material parameters the Equation (7.1) is approximated by a polynomial of the elastic parameters of the cell wall. The dependency is determined for a range of values of the chosen parameters $\Xi = \{E_1, E_2, G_{12}, G_{23}\}$ given in Table 7.3. All other parameters are given the mean values of Tables 7.2 and 7.3, excluding Poisson's ratios that are given value 0.3. The simplest possible fit is used that fulfills a case dependent approximation error criteria, for which a more detailed explanation is given in Publication IV.

For a dimensionless representation, a mean value of the modulus of elasticity E_2 is used as the reference quantities in the calculations. The effect of the elastic parameters as linear function is

$$\begin{Bmatrix} E_R/E_2 \\ E_T/E_2 \\ E_L/E_2 \\ G_{RT}/E_2 \\ G_{RL}/E_2 \\ G_{TL}/E_2 \\ \nu_{RT} \\ \nu_{LR} \\ \nu_{LT} \end{Bmatrix} = \begin{bmatrix} 0 & 0.0284 & 0.0459 & 0.0382 \\ 0 & 0.0142 & 0.0153 & 0.0516 \\ 2.26 & 0 & 0 & 0 \\ 0 & 0.00284 & 0.00228 & 0.0127 \\ 0 & 0 & 0.0070 & 0.137 \\ 0 & 0 & 0.0912 & 0.0300 \\ 0.692 & 0.0714 & 0 & 0 \\ 0.298 & 0 & 0 & 0 \\ 0.298 & 0 & 0 & 0 \end{bmatrix} \begin{Bmatrix} 1 \\ E_1/E_2 \\ G_{12}/E_2 \\ G_{23}/E_2 \end{Bmatrix}. \tag{7.3}$$

The polynomial relationship was found to give a representation within a defined error, which was between 1% and 2% depending on the case.

If a more accurate approximation is needed, the domain for the varied parameters can be divided into several subdomains. By dividing the area into eight subdomains and using a linear fit, the error could be decreased to below 1%.

As would be expected, E_L in the out-of-plane -direction ν_{LR} and ν_{LT} did not depend on the cell wall material parameters. This follows the cell wall material parameters where $E_3 > E_2$, $E_3 > E_1$.

7.6.2 Effect of thickness

The only varying parameter for this example is the thickness of a cell wall for earlywood, which limits the parameters to $\Upsilon = \{t\}$. Other parameters are again given their mean values. In the calculations a range $t \in [0.0007, 0.0027]$ mm is used. For a dimensionless representation, the earlywood cell width w_e=0.0236 mm is used as the reference quantities in the calculations. An example on the dependency of the rigidity on thickness in earlywood is shown in Figures 7.2, 7.3, 7.4, and 7.5 for different values of E_1/E_2.

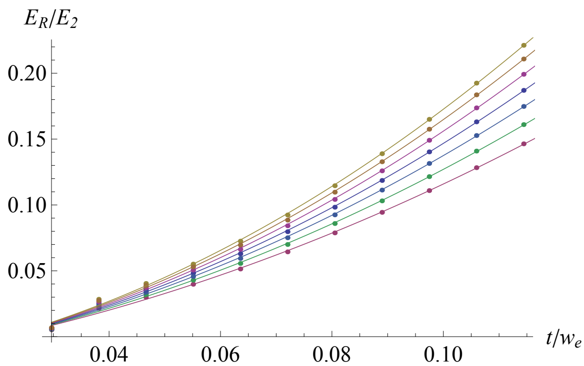

Figure 7.2. E_R/E_2 as function of t, shown for values $E_1 \in \{1, 1.17, 1.34, 1.5, 1.67, 1.84, 2\}$ from lowest to highest curve.

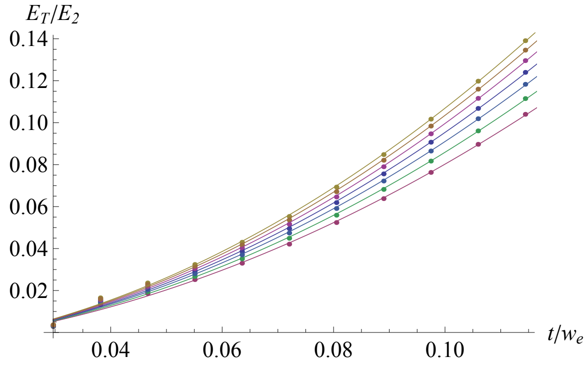

Figure 7.3. E_T/E_2 as function of t, shown for values $E_1 \in \{1, 1.17, 1.34, 1.5, 1.67, 1.84, 2\}$ from lowest to highest curve.

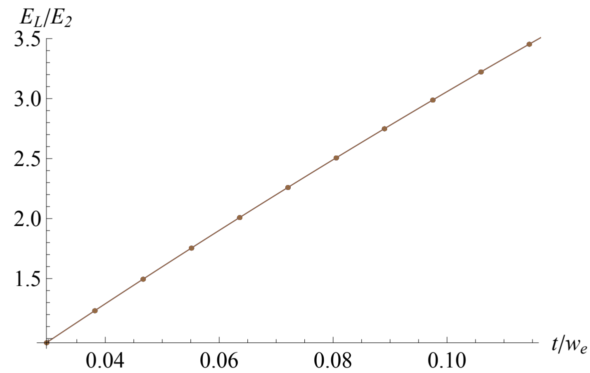

Figure 7.4. E_L/E_2 as function of t, coinciding curves are shown for values $E_1 \in \{1, 1.17, 1.34, 1.5, 1.67, 1.84, 2\}$.

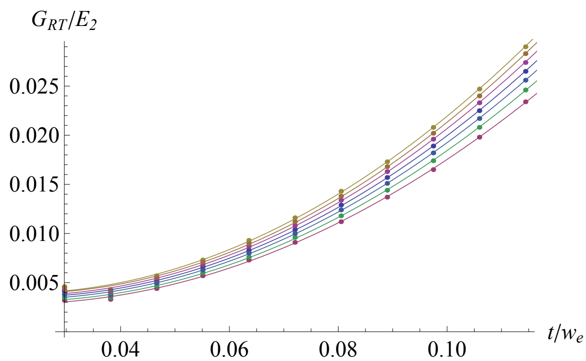

Figure 7.5. G_{RT}/E_2 as function of t, shown for values $E_1 \in \{1, 1.17, 1.34, 1.5, 1.67, 1.84, 2\}$ from lowest to highest curve.

Third order polynomial of the thickness is selected, shown as the middle line in Figures 7.2, 7.3, 7.4, and 7.5. The polynomial is

$$\begin{Bmatrix} E_R/E_2 \\ E_T/E_2 \\ E_L/E_2 \\ G_{RT}/E_2 \\ G_{RL}/E_2 \\ G_{TL}/E_2 \\ \nu_{RT} \\ \nu_{LR} \\ \nu_{LT} \end{Bmatrix} = \begin{bmatrix} 0 & -0.181 & 21.6 & -50.6 \\ 0 & -0.008 & 9.60 & 0 \\ 0.124 & 29.4 & 0 & 0 \\ 0.001 & 0.065 & 0 & 12.1 \\ 0 & 0.822 & 0 & 0 \\ 0 & 0.756 & 0 & 0 \\ 2.07 & -40.1 & 434 & -1750 \\ 0.298 & 0 & 0 & 0 \\ 0.298 & 0 & 0 & 0 \end{bmatrix} \begin{Bmatrix} 1 \\ t/w_e \\ (t/w_e)^2 \\ (t/w_e)^3 \end{Bmatrix}. \tag{7.4}$$

Similar to material parameters, E_L in the out-of-plane -direction was linear in t and ν_{LR} and ν_{LT} were constant. The effective elasticity dependency on thickness in earlywood shown for example in Figures 7.2, 7.3, 7.4, and 7.5 shows the effect of cell wall thickness. As expected, the effective RT-plane stiffness parameters were the most complex and depended strongly on the thickness of the cell wall.

7.6.3 Effect of transition-/latewood parameter

The growth ring becomes important if wood is studied at a larger scale. The cells become more narrow and the cell walls thicker in transition- and latewood. To quantify this behaviour of the cell narrowing using just one parameter with the structural element of three vectors is not possible. This is why a hexagonal structural element shown in Figure 3.3 is chosen. All geometric parameters affected by the transition-/latewood are tied to the width of the structural element.

To find the effective rigidity in transition-/latewood, a parameter describing the location in the growth ring r is used. The structure of the transition-/latewood is found from spruce specimens and literature (Havimo et al. 2008, Persson 2000). Transition- and latewood are assumed to take 20% of the width of the growth ring (Rafsanjani et al. 2012, Rosner et al. 2007). The cell width and wall thickness of transition and latewood

$$w = w_e(3.36 - 2.95 * r) \qquad 0.8 \leq r \leq 1, \tag{7.5}$$

$$t = t_e(-3.88 + 6.10 * r) \qquad 0.8 \leq r \leq 1, \tag{7.6}$$

are linear with respect to the relative radial cell location in the growth ring $r \in [0, 1]$. The thickness is $t_e = 0.0017$ mm and width $w_e = 0.0236$ mm.

The coefficients were calculated by analysing images of spruce growth rings. Then the parameter of the rigidity is $\Upsilon = \{r\}$ and again all other parameters are given their mean values. An example on the dependency of rigidity in transition-/latewood is shown in Figures 7.6, 7.7, 7.8, and 7.9.

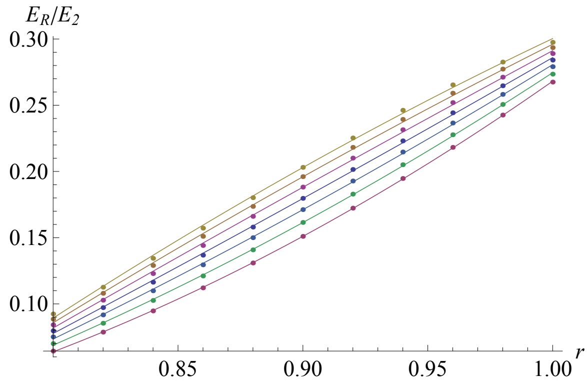

Figure 7.6. E_R/E_2 as function of r, shown for values $G_{12} \in \{0.25, 0.32, 0.39, 0.45, 0.52, 0.59, 0.65\}$ from lowest to highest curve.

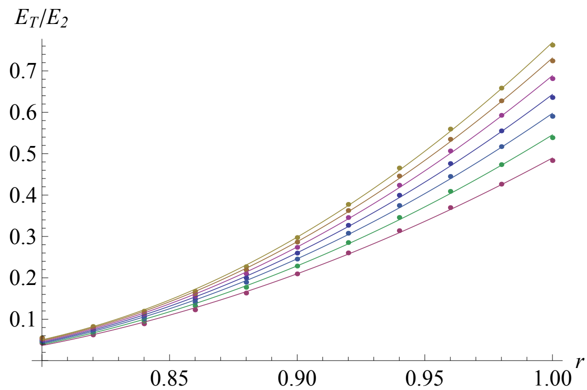

Figure 7.7. E_T/E_2 as function of r, shown for values $G_{12} \in \{0.25, 0.32, 0.39, 0.45, 0.52, 0.59, 0.65\}$ from lowest to highest curve.

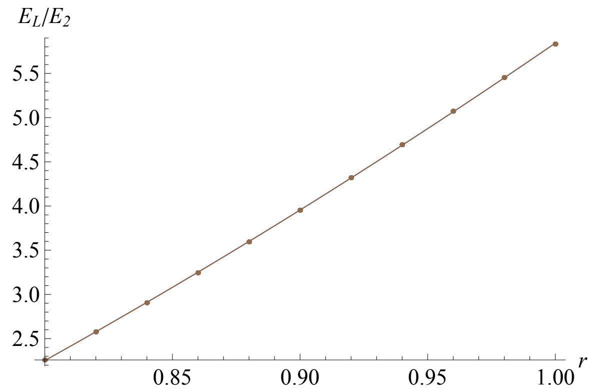

Figure 7.8. E_L/E_2 as function of r, coinciding curves are shown for values $G_{12} \in \{0.25, 0.32, 0.39, 0.45, 0.52, 0.59, 0.65\}$.

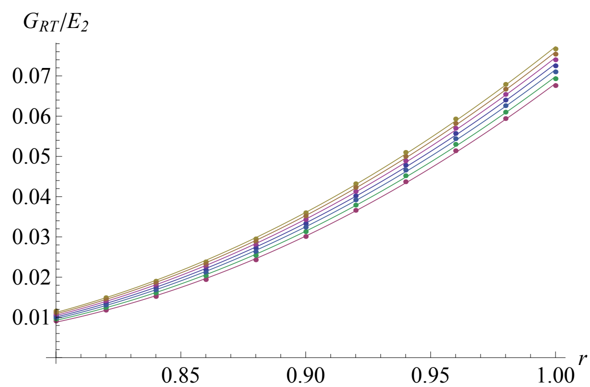

Figure 7.9. G_{RT}/E_2 as function of r, shown for values $G_{12} \in \{0.25, 0.32, 0.39, 0.45, 0.52, 0.59, 0.65\}$ from lowest to highest curve.

Third order polynomial was selected for the relative location in the growth ring, $r \in [0.8, 1]$ shown as the middle line in Figures 7.6, 7.7, 7.8, and 7.9. The polynomial is

$$\begin{Bmatrix} E_R/E_2 \\ E_T/E_2 \\ E_L/E_2 \\ G_{RT}/E_2 \\ G_{RL}/E_2 \\ G_{TL}/E_2 \\ \nu_{RT} \\ \nu_{LR} \\ \nu_{LT} \end{Bmatrix} = \begin{bmatrix} -0.760 & 1.05 & 0 & 0 \\ 22.2 & -71.9 & 75.0 & -24.7 \\ -12.2 & 18.0 & 0 & 0 \\ 1.55 & -4.98 & 5.08 & -1.58 \\ -0.452 & 0.744 & 0 & -0.167 \\ 0.845 & -2.46 & 1.85 & 0 \\ 39.5 & -110 & 102 & -31.7 \\ 0.296 & 0 & 0 & 0 \\ 0.299 & 0 & 0 & 0 \end{bmatrix} \begin{Bmatrix} 1 \\ r \\ r^2 \\ r^3 \end{Bmatrix}. \tag{7.7}$$

The parameter r shows the combined effect of cell shape (width of the cell) and thickness of the cell wall. For r in for example Figures 7.6, 7.7, 7.8, and 7.9, the values of rigidity had a larger range than the ones for only thickness. Also the polynomial dependency was more complex for r than t. This was probably due to cell walls becoming quite thick as r approaches 1, which showed behaviour not present for smaller thickness values.

7.7 Discussion

A spruce cell material was modeled with the methods of Chapters 3, 4 and 5. The aim was to find the effective rigidity of a spruce specimen as function of the geometric and elastic parameters. For a regular structure, the method of Chapter 5 gives the rigidity for any combination of the geometric and cell wall parameters and thereby for any specimen of the growth ring, for example in any point of the image on the left of Figure 2.4, assuming that the scale of variation of the parameters is slow compared to the cell size. Also the relative effect of the parameters was studied to find the most significant parameters.

The method of Chapter 3 was used to analyse and generate the geometry of spruce. The method used a reference structural element and mapping to find the geometry in a statistical sense. The requirement of connectivity for the structural element made it impossible to include all vertex points into the analysis, but on the other hand the method gave a short description including the variation.

The rigidity simulation method of Chapter 4 was used to study the effect of variation to rigidity. The difference measures, e, for image case given in Table 7.5 varied greatly from specimen to specimen. This could be due to different kinds of organized features in the image geometry, such as rays, which appear as a row on thicker cell walls or as a row of relatively large or small cells. One problem was the small size of the wood images, which restricted the size of the image specimens and gave quite large variations for the parameters. Also, the problem for calculating the compliance of the image case had to do with defining the boundaries of the domain. Unfortunately, the size was so small that the boundaries had an effect on the results for the image case.

The effect of the thickness variation Stat. (ρ) in Table 7.4 was found to be particularly strong between 64% and 110% for large-sized specimens and for Table 7.5 between 50% and 85% for small-sized specimens. Therefore no variation and only the mean value of the thickness may give a quite erroneous result. The use of the mean thickness in the simulations underestimates the rigidity of the structure.

Computational homogenization method on a regular cell structure in Chapter 5 was used to quantify the effect of cell geometry and cell wall material properties on the effective rigidity properties. The sensitivity calculations indicate that the important parameters to include were limited to five. With the method any combination of the parameters could be used to calculate the effective rigidity.

The homogenization method assumes a regular structure but could include details such as the growth ring when calculated in pieces, assuming that the change in the parameters is assumed much larger than the cell size. The structures can be modeled as a change in the mean values of the parameters and again the specimens forming the entire structure can be assumed to be regular. For small variation or large specimens the homogenization model and the orthotropic cell wall material give the best description of spruce.

8. Conclusions

Rigidity of cellular structure depends on multiple geometric and cell wall elastic parameters. The experimental effort in understanding the behaviour of cellular structures can be reduced if a qualitative understanding on the behaviour is first obtained by simulation. Simulation tool is also important when the cell wall properties are sought by an indirect experimental method where the parameters of simulation experiments are tuned so that the effective properties match with physical experiments. In addition, modeling offers the possibility of separating different parameters in an effort to recognize the most important ones.

For analysing non-regular geometries, a geometric model was introduced. The starting point in finding the geometry was a scanned image of Nomex or spruce from which the image geometry is found. A concept of structural element was used to analyse the geometry in a statistical sense. The exactly same method can be used to generate a statistically equivalent geometry for modeling.

Rigidity simulation was used to find the properties of a non-regular structure. The method utilized a beam model for the individual cell walls and gave the compliance of the structure. The drawback of the model is the large computational effort required and effect of the boundaries.

A regular structure was considered by means of computational homogenization. The method gave the effective rigidity of the regular cell structure for any type of structural element. Closed form expressions based on particle model and cell-type structural elements were obtained which illustrated the effect of individual parameters on rigidity.

A simplified model of wood, namely Nomex, was used to validate the used beam model by comparing the results of two different cell structures. Physical and simulation experiments on a large scale were matched to find the elastic parameter of the cell wall in the micro scale.

The variation of geometric and elastic cell wall parameters in spruce was considered by using a rigidity simulation. A sensitivity measure of rigidity was calculated for the variation. As a result, the effect of thickness variation was found to be significantly larger than the effect of geometry or cell wall parameter variation.

Computational homogenization method was applied to a regular spruce specimen, where the structural element was a cell type prism with orthotropic cell walls. As a result the rigidity of spruce could be calculated for any values of the geometric and cell wall elastic parameters.

In order to see when Bernoulli beams can be used for different wall thickness values, the homogenization method is used for both orthotropic cell walls and beam cell walls. When the values are calculated for the analytical method with elastic modulus $E = E_1 = 1.5$ GPa and geometric values given before. The values E_T/E_2 as a function of t or r are given in Figures 8.1 and 8.2 for beam model in purple and linear-elastic model in blue. The results show that a beam approximation may give relatively accurate values for the rigidity of a wood cell structure for small thickness values as in earlywood.

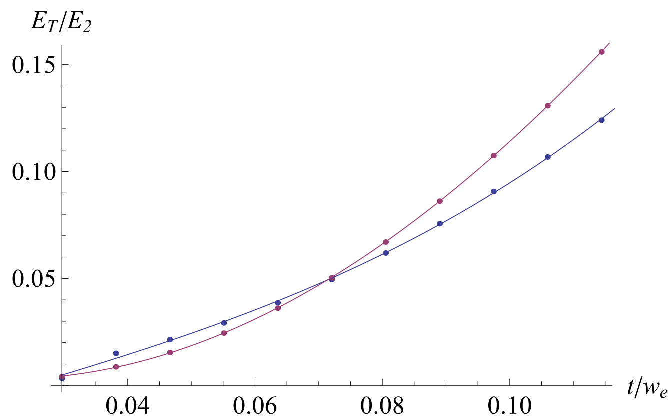

Figure 8.1. E_T/E_2 as function of t, the beam model in purple and the linear-elastic model in blue. Material parameters are given mean values.

The method was limited by specimen size and ignored features such as rays. In order to improve the method, omitted features could be included and larger specimens with better accuracy could be used. This would make it possible find data directly on whole growth rings.

In the present study, the finest level of modelling was chosen to be cell wall of homogeneous orthoropic material. In step towards a more detailed model, the layered structure of the cell wall could be included. The cell

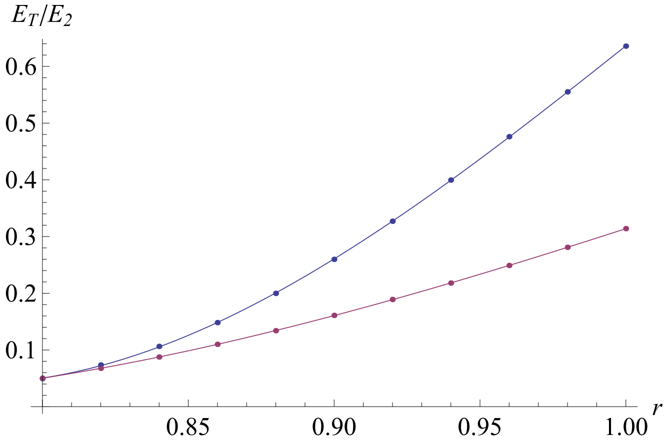

Figure 8.2. E_T/E_2 as function of r, the beam model in purple and the linear-elastic model in blue. Material parameters are given mean values.

wall layers could be modeled for example as cellulose fibres embedded in a matrix of hemicellulose and either pectin or lignin.

In order to improve the study of variation, two methods could be developed. One would use a quasi non-regular structure, where the structural element of a regular structure would be a small non-regular specimen. In this method the computational effort may become restrictive. Another method would be to calculate the rigidity of a mechanically continuous non-regular beam structure so that the effect of boundaries would be reduced. Comparing these results to the results of a regular structure would give a better estimation on the accuracy of the different models.

Bibliography

Astley, R. J., Stol, K. A. & Harrington, J. J. (1998), 'Modelling the elastic properties of softwood', *European journal of wood and wood properties* **56**, 43–50.

Bergander, A. & Salmén, L. (2000), 'Variations in transverse fibre wall properties: relations between elastic properties and structure', *Holzforschung* **54**, 654–660.

Bergman, R., Cai, Z., Carll, C. G., Clausen, C. A., Dietenberger, M. A., Falk, R. H., Frihart, C. R., Glass, S. V., Hunt, C. G., Ibach, R. E., Kretschmann, D. E., Rammer, Douglas R.and Ross, R. J., Stark, N., Wavker, J. P., Wang, X., White, R. H., Wiedonhoeft, A. C., Wiemann, M. C. & Zelinka, S. L. (2010), Wood handbook, wood as an engineering material, Technical report, Madison, WI: U.S. Department of Agriculture, Forest Service, Forest Products Laboratory.

Boas, M. L. (1983), *Mathematical methods in the physical sciences*, second edn, John Wiley and sons.

Bovik, A. (2005), *Handbook of image and video processing*, second edn, Elsevier Academic Press.

Charalambakis, N. (2010), 'Homogenization techniques and micromechanics. A survey and perspectives', *Applied Mechanics Reviews* **63**(3), 030803.

Chen, D. H. (2010), 'Bending deformation of honeycomb consisting of regular hexagonal cells', *Composite Structures* **93**, 736–746.

Chen, D. H. & Osaki, S. (2009), 'Analysis of in-plane elastic modulus for a hexagonal honeycomb core: Effect of core height and proposed analytical method', *Composite Structures* **88**, 17–25.

Chung, K.-L., Huang, Y.-H., Wang, J.-P., Chang, T.-C. & Mark Liao, H.-Y. (2010), 'Fast randomized algorithm for center-detection', *Pattern Recognition* **43**, 2659–2665.

Eringen, A. C. (1999), *Microcontinuum field theories: I. Foundations and solids*, first edn, Springer Verlag.

Fazekas, A., Dendievel, R., Salvo, L. & Bréchet, Y. (2002), 'Effect of microstructural topology upon the stiffness and strength of 2D cellular structures', *International Journal of Mechanical Sciences* **44**, 2047–2066.

Foo, C. C., Chai, G. B. & Seah, L. K. (2007), 'Mechanical properties of Nomex material and Nomex honeycomb structure', *Composite Structures* **80**, 588–594.

Foo, C. C., Chai, G. B. & Seah, L. K. (2008), 'A model to predict low-velocity impact response and damage in sandwich composites', *Composite Science and Tehnology* **68**, 1348–1356.

Gibson, L. J. & Ashby, M. F. (1997), *Cellular solids: Structure and properties*, second edn, Camdridge University Press.

Gonella, S. & Ruzzene, M. (2008), 'Homogenization and equivalent in-plane properties of two-dimensional periodic lattices', *International Journal of Solids and Structures* **45**, 2897–2915.

Harrington, J., Astley, R. & Booker, R. (1998), 'Modelling the elastic properties of softwood', *Holz als Roh-und Werkstoff* **56**(1), 37–41.

Hassani, B. & Hinton, E. (1998), 'A review of homogenization and topology optimization I—homogenization theory for media with periodic structure', *Computers & Structures* **69**(6), 707–717.

Havimo, M., Rikala, J., Sirviö, J. & Sipi, M. (2008), 'Distributions of tracheid cross-sectional dimensions in different parts of Norway spruce stems', *Silvia Fennica* **49**, 89–99.

Hofstetter, K. & Gamstedt, E. K. (2009), 'Hierarchical modelling of microstructural effects on mechanical properties of wood. a review COST Action E35 2004–2008: Wood machining–micromechanics and fracture', *Holzforschung* **63**(2), 130–138.

Hohe, J. & Becker, W. (2000), 'A mechanical model for two-dimensional cellular sandwich cores with general geometry', *Computational Materials Science* **19**, 108–115.

Hohe, J. & Becker, W. (2002), 'Effective stress-strain relations for two-dimensional cellular sandwich cores: Homogenization, material models, and properties', *Applied Mechanics Reviews* **55**(1), 61–87.

Hohe, J., Beschorner, C. & Becker, W. (1999), 'Effective elastic properties of hexagonal and quadrilateral grid structures', *Composite Structures* **46**(1), 73–89.

Holmberg, S., Persson, K. & Petersson, H. (1999), 'Nonlinear mechanical behaviour and analysis of wood and fibre materials.', *Computers and Structures* **72**, 459–480.

Hugh, J. (1976), *The international book of wood*, first edn, Mitchell Beazley.

Jäger, A., Bader, T., Hofstetter, K. & Eberhardsteiner, J. (2011), 'The relation between indentation modulus, microfibril angle, and elastic properties of wood cell walls', *Composites Part A: Applied Science and Manufacturing* **42**(6), 677–685.

Kahle, E. & Woodhouse, J. (1994), 'The influence of cell geometry on the elasticity of softwood', *Journal of Materials Science* **72**, 459–480.

Karakoç, A. & Freund, J. (2012), 'Experimental studies on mechanical properties of cellular structures using Nomex® honeycomb cores', *Composite Structures* **94**(6), 2017–2024.

Karakoç, A., Santaoja, K. & Freund, J. (2013), ‘Simulation experiments on the effective in-plane compliance of the honeycomb materials’, *Composite Structures* **96**, 312–320.

Karlsson, K. F. & Aström, B. T. (1997), ‘Manufacturing and applications of structural sandwich components’, *Composites: Part A* **28A**, 91–111.

Khedr, A. M. & Salim, A. (2008), ‘Decomposable algorithms for nearest neighbor computing’, *J. Parallel Distrib. Comput.* **68**, 902–912.

Koponen, S., Toratti, T. & Kanerva, P. (1991), ‘Modelling elastic and shrinkage properties of wood based on cell structure’, *Wood science and technology* **25**(1), 25–32.

Meraghni, F., Desrumaux, F. & Benzeggagh, M. L. (1999), ‘Mechanical behaviour of cellular core for structural sandwich panels’, *Composites: Part A* **30**, 767–779.

Mishnaevsky, Jr., L. & Qing, H. (2008), ‘Micromechanical modelling of mechanical behaviour and strenght of wood: State-of-the-art review.’, *Computational Materials Science* **44**, 363–370.

Modén, C. S. & Berglund, L. (2008), ‘A two-phase annual ring model of transverse anisotropy in softwoods’, *Composites Science and Technology* **68**(14), 3020–3026.

Narendra, P. M. & Fukunaga, K. (1977), ‘A branch and bound algorithm for feature subset selection’, *IEEE Transactions on Computers* **26**, 917–922.

Nguyen, V.-D., Béchet, E., Geuzaine, C. & Noels, L. (2012), ‘Imposing periodic boundary condition on arbitrary meshes by polynomial interpolation’, *Computational Materials Science* **55**, 390–406.

Noor, A. K., Burton, W. S. & Bert, C. W. (1996), ‘Computational models for sandwich panels and shells’, *Applied Mechanics Reviews* **49**(3), 155–199.

Persson, K. (2000), Micromechanical modelling of wood and fibre properties., PhD thesis, Lund university.

Qing, H. & Mishnaevsky Jr, L. (2010), ‘3D multiscale micromechanical model of wood: From annual rings to microfibrils’, *International Journal of Solids and Structures* **47**(9), 1253–1267.

Qing, H. & Mishnaevsky, L. (2011), ‘A 3D multilevel model of damage and strength of wood: Analysis of microstructural effects’, *Mechanics of Materials* **43**(9), 487–495.

Rafsanjani, A., Derome, D. & Carmeliet, J. (2012), ‘The role of geometrical disorder on swelling anisotropy of cellular solids’, *Mechanics of Materials* **55**, 49–59.

Rosner, S., Klein, A., Müller, U. & Karlsson, B. (2007), ‘Hydraulic and mechanical properties of young Norway spruce clones related to growth and wood structure’, *Tree physiology* **27**(8), 1165–1178.

Sarèn, M.-P., Serimaa, R., Andersson, S. & Paakkari, T. (2001), ‘Structural variation of tracheids in Norway spruce (*Picea abies* (l.) karst.)’, *Journal of structural biology* **136**, 101–109.

Schwingshackl, C. W., Aglietti, G. S. & Cunningham, P. R. (2006), 'Determination of honeycomb material properties: existing theories and an alternative dynamic approach', *Journal of aerospace engineering* **19**(3), 177–183.

Sedighi-Gilani, M. & Navi, P. (2007), 'Experimental observations and micromechanical modeling of successive-damaging phenomenon in wood cells' tensile behavior', *Wood science and technology* **41**(1), 69–85.

Silva, M. J. & Gibson, L. J. (1995), 'The effects of non-periodic microstructure on the elastic properties of two-dimensional cellular solids', *International Journal of Mechanical Sciences* **37**, 1161–1171.

Wang, A.-J. & McDowell, D. L. (2004), 'In-Plane Stiffness and Yield Strength of Periodic Metal Honeycombs', *Journal of Engineering Materials and Technology* **126**.

Watanabe, U., Fujita, M. & Norimoto, M. (2002), 'Transverse Young's moduli and cell shapes in coniferous early wood', *Hozforschung* **56**, 1–6.

Wittel, F. K., Dill-Langer, G. & H., K. B. (2005), 'Modeling of damage evolution in soft-wood perpendicular to grain by means of discrete element approach', *Computational Materials Science* **32**, 594–603.

Zhu, H. X., Hobdell, J. R. & Windle, A. H. (2001), 'Effects of cell irregularity on the elastic properties of 2D Voronoi honeycombs', *Journal of the Mechanics and Physics of Solids* **49**, 857–870.

Zienkiewich, O. C. & Taylor, R. L. (2002), 'Transverse Young's moduli and cell shapes in coniferous early wood.', *Holzforschung* **56**, 1–6.

Wood is an abundant, durable and economical natural product that is inherently orthotropic and inhomogeneous. It is widely used in applications, ranging from construction to pulping. The structure of wood consists of long cells, which have random variation of shape and size, but also directed variation due to the growth ring. The mechanical properties of wood depend on geometry of the cell structure, thickness and elastic properties of a cell wall.
Physical experiments on rigidity give only a general idea of the behaviour of a material. Simulation experiments based on micromechanical modeling give a freedom of design and different features can be considered individually. In this work the relative effect of geometric and material features on rigidity of wood is quantified, which gives insight into their importance. A model is developed that can be used to calculate the effective rigidity for any location in the growth ring.

Aalto-DD 38/2015

ISBN 978-952-60-6132-0 (printed)
ISBN 978-952-60-6133-7 (pdf)
ISSN-L 1799-4934
ISSN 1799-4934 (printed)
ISSN 1799-4942 (pdf)

Aalto University
School of Engineering
Department of Applied Mechanics
www.aalto.fi

BUSINESS +
ECONOMY

ART +
DESIGN +
ARCHITECTURE

SCIENCE +
TECHNOLOGY

CROSSOVER

DOCTORAL
DISSERTATIONS